Universidade de Aveiro Departamento de Química
2018

Cristiana Areia dos Santos

Separação de compostos bioactivos recorrendo à tecnologia de leito móvel simulado

Bioactive compounds separation with Simulated Moving Bed technology

Universidade de Aveiro Departamento de Química
2018

Cristiana Areia dos Santos

Separação de compostos bioactivos recorrendo à tecnologia de leito móvel simulado

Bioactive compounds separation with Simulated Moving Bed technology

Dissertação apresentada à Universidade de Aveiro para cumprimento dos requisitos necessários à obtenção do grau de Mestre em Engenharia Química, realizada sob orientação científica de Doutor Carlos Manuel Santos da Silva, Professor Associado do Departamento de Química da Universidade de Aveiro e da Doutora Maria Inês Purcell de Portugal Branco, Professora Auxiliar do Departamento de Química da Universidade de Aveiro.

In memoriam do meu primo, Joel.

O júri / The jury

Presidente / President

Prof. Doutor Francisco Avelino da Silva Freitas
Professor Auxiliar do Departamento de Química da Universidade de Aveiro

Vogais / Committee

Doutor António Augusto Areosa Martins
Investigador Pós-Doutoramento no Laboratório de Engenharia de Processos, Ambiente, Biotecnologia e Energia da Faculdade de Engenharia da Universidade do Porto da Universidade do Porto

Prof. Doutor Carlos Manuel Santos da Silva
Professor Associado do Departamento de Química da Universidade de Aveiro

Agradecimentos / Acknowledgements

Quero expressar o meu agradecimento ao professor Carlos Manuel Silva, meu orientador, por esta oportunidade de trabalhar no grupo EgiChem, disponibilidade e atenção.

De igual forma agradeço à minha co-orientadora, a professora Inês Portugal, pelas vezes que se mostrou disponível e pelas palavras ao longo do curso.

Ao grupo EgiChem, por me terem acolhido desde o primeiro dia, estou deveras agradecida.

Ao Ivo Azenha e ao José Pedro Aniceto por sempre se mostrarem prestáveis em ajudar, muitíssimo obrigada pelo conhecimento transmitido.

À Doutora Mónica Valéga, muito obrigada por toda ajuda dada ao longo desta dissertação.

Muito obrigada aos meus amigos que me acompanharam durante o meu percurso académico, por todos os bons momentos e todo apoio que me proporcionaram, estarão sempre no meu coração.

A minha profunda gratidão aos meus pais, irmão, assim como aa restante família, que sempre me apoiaram e que são a principal base da minha educação.

Palavras-chave

ácidos triterpénicos; adsorção; cromatografia líquida de alto desempenho; curvas de rutura; isotérmica; leito móvel simulado; separação;

Resumo

No último meio século, os produtos naturais tem sido gradualmente esquecidos pelas maiores companhias de investigação farmacêuticas como fontes de novos medicamentos. Porém atualmente observou-se uma mudança de estratégia que promoveu um novo interesse na integração dos produtos naturais nestes. Os ácidos triterpénicos fazem parte de um grupo promissor de metabolitos secundários que podem ser encontrados em plantas, flores, folhas com grande variedade de benficios. Nesta dissertação estudou-se o isolamento dos ácidos oleanólico e ursólico por técnicas cromatográficas, recorrendo à tecnologia de leito móvel simulado (SMB). A separação dos ácidos triterpénicos é complexa dada à sua semelhança estrutural. No laboratório do grupo EgiChem (CICECO, UA) está a ser instalada uma unidade de SMB, porém é necessário realizar ensaios preliminares para selecionar a fase móvel mais adequada, bem como a otimização das condições de operação de ambos os ácidos. Posto isto, analisou-se a influência do solvente/mistura de solventes na separação cromatográfica recorrendo à medição de seletividades, factores de retenção e resolução. Foi testada uma coluna triacontyl (Acclaim C30), sendo que os melhores resultados foram obtidos com a fase móvel metanol/água 95/5 (%, v/v). Seguiu-se à medição das curvas de rutura de modo a determinar os parametros de processo como as isotérmicas de equilibrio (constantes H_i) do ácido oleanólico e do ácido ursólico, e os coeficientes globais de transferência de massa do modelo da força motriz linear ($K_{LDF,i}$). Os dados obtidos foram modelados através da equação de Klinkenberg, que é aplicado especificamente para sistemas lineares. As constantes de equilíbrio linear dos ácidos oleanólico e ursólico foram H_{OA}= 2.06 e H_{UA}= 2.16, respetivamente, e os coeficientes globais de transferência de massa LDF de $K_{LDF,OA}$= 30.48 min^{-1} e $K_{LDF,UA}$= 101.45 min^{-1} com desvios médios de $AADR_{OA}$=18.29 % e $AADR_{UA}$=26.88 %. Por fim foi realizada uma simulação de uma unidade SMB para a separação de uma mistura de ácidos oleanólico e ursólico, com uma configuração 2-2-2-2, usando o enchimento da coluna Acclaim C30 e a fase móvel metanol/água 95/5 (%, v/v) e os parâmetros de equilibrio e cinética otimizados anteriormente. Os resultados obtidos para esta configuração mostraram que é possível produzir correntes purificadas de cada ácido com concentrações acima dos 99%.

Keywords adsorption; breaktrhough curves; isotherms; high performance liquid chromatography; triterpenic acids; separation; simulated moving bed.

Abstract

Natural products have been progressively forgotten by major pharmaceutical research companies as sources for new drugs in the last half century. Currently one observes a change of strategy, which is promoting a renewed interest on the integration of natural products into pharmaceuticals. Triterpenic acids are a promising group of plant secondary metabolites occurring in cuticular waxes covering fruits, flowers, and leaves, providing a wide variety of beneficial biological activities. In this dissertation it was studied the oleanolic and ursolic acids isolation by chromatographic tecnique of simulated moving bed (SMB). The seperation of triterpenic acids is complex due their similar structure. EgiChem laboratory (CICECO, UA) has a SMB unit, but it is necessary to carry out preliminary experiments in order to select the best mobile phase and optimal operating conditions for separation of both acids. For that, it was analyzed the infuence of the solvent/mixture of solvents on the chromatographic separation by measuring selectivity, retention factor and resolution. It was tested a triacontyl column (Acclaim C30), and the best results were obtained with a mobile phase of methanol/water 95/5 (%, v/v). Then, breakthrough curves have been measured in order to determine process parameters like the equilibrium isotherms (constants H_i) of both oleanolic and ursolic acids, and the global linear driving force (LDF) coefficients of mass transfer ($K_{LDF,i}$). Data modeling was accomplished using Klinkenberg equation, which is specifcially applicable to linear systems. The equilibrium constants of oleanolic and ursolic acdis were H_{OA}= 2.06 and H_{UA}= 2.16, respectively, and global LDF coefficients were $K_{LDF,OA}$= 30.48 min^{-1} and $K_{LDF,UA}$= 101.45 min^{-1} with average deviaions of $AADR_{OA}$=18.29 % and $AADR_{UA}$=26.88 %. Finally the simulation of a SMB unit for a oleanolic/ursolic acids mixture separation was accomplished, with a 2-2-2-2 configuration, using the packing of Acclaim C30 column and methanol/water 95/5 (%, v/v) as mobile phase and the equilibrium and kinetic parameters previously optimized. The obtained results for configuration showed that the separation of oleanolic and ursolic acids is viable, being possible to produce purified streams of each acid with concentrations above 99%.

Contents

List of Tables

List of Figures

Nomenclature

$AARD$ - Average absolute relative deviation
b_{i} - Equilibrium constant of the compound
$C_{\mathrm{i}}{}^{*}$ - Equilibrium concentration with $\overline{q_i}$. $(mg \cdot mL^{-1})$
C_{ij} - Liquid phase concentration $(mg \cdot mL^{-1})$
d_{p} - Particle diameter (mm)
D_{ax} - Axial dispersion $(cm^2 \cdot min^{-1})$
D_{eff} - Effective diffusion coefficient $(cm^2 \cdot min^{-1})$
$D_{\mathrm{m,i}}$ - Molecular diffusion coefficient $(cm^2 \cdot min^{-1})$
H_{i} - Equilibrium constant
$K_{\mathrm{LDF,i}}$ - global linear driving force coefficient of mass transfer (min^{-1})
$k^{'}$ - Retention time factor
L_{c} - Length of column (cm)
M_{f} - Molecular weight of the solvent $(g \cdot mol)$
m_{j} - Ratio between fluid and solid flow rates
NDP - Number of data points
$Prod$ - Productivity $(kg \cdot m^3{}_{adsorbent} \cdot day)$
Pur - Purity (%)
q_{i} - Solid phase concentration $(mg \cdot mL^{-1})$
$\overline{q}$ - Average concentration of solid phase $(mg \cdot mL^{-1})$
q^{*} - Solid phase concentration in equilibrium with liquid phase $(mg \cdot mL^{-1})$
Q_{i} - Flow rate $(mL \cdot min^{-1})$
Q - Adsorbent capacity
R - Resolution
Rec - Recovery (%)
S - Solubility $(g \cdot mL^{-1})$
SC - Solvent consumption
t^{*} - Switching time (min)
T - Absolute temperature (K)
t - Time (min)
t_{r} - Retention time (min)

u_{i} - Linear velocity ($m \cdot s^{-1}$)
u_{s} - Solid velocity ($m \cdot s^{-1}$)
V_{c} - Column volume (cm^3)
V_{critical} - Critical volume (cm^3)
V_{S} - Volume of solvent (mL)
$V_{\mathrm{bp,i}}$ - Solute molar volume at its normal boiling point ($cm^3 \cdot mol$)
v^*_{j} - Liquid velocity in SMB ($m \cdot s^{-1}$)
W_{v} - Weighed glass vial mass (g)
W_{VR} - Mass of the glass vial and the residue (g)
$w_{1/2}$ - Half width of the elution peak
z - Position variable (m)

Greek letters

α - Selectivity
β -Safety merge
ε - Bed porosity
φ - Dimensionless distance
τ - Displacement-corrected time
λ - Wavelength (nm)
ϕ - Dimensionless association factor for the solvent
μ_{f} - Solvent viscosity (cP)
ρ_{f} - Fluid density

Subscripts and superscripts

I, II, III, IV - SMB and TMB sections
c - Column
calc - Calculated values
exp - Experimental values
F - Feed
i - Compound
j - Column
R - Raffinate
X - Extract

1 Introduction

The demand for energy and fuels is growing, jointly with the declining of fossil fuels reserves and the increase of environmental problems caused by them, prioritized the search for new sustainable resources in the last decades.

Biomass, the organic material derived from living matter, seems to be a promising option to improve the environmental situation by taking advantage of other additional positive effects, and has emerged as key source of a wide variety of fine chemicals [1; 2]. In this way, biorefinery integrates the process of biomass conversion to produce fuels, power and chemicals. Nature provides an enormous variety of resources that can be converted into functional materials [3].

By using green chemical technologies and designing processes for maximum conversion efficiencies and minimal waste, make the products of biorefinery green and sustainable [4; 5].

Although natural products have been progressively forgotten by major pharmaceutical research companies as sources for new drugs over the past half century, there is a change of strategy, which is promoting a renewed interest on the integration of natural products into the pharmaceuticals R&D, as well as on the development of innovative nutraceutics and cosmetics [6].

One of the most successful examples is the exploitation of pulp industries by-products. Without affecting the current most important outputs of the existent mills, this concept may lead to the generation of valuable products while minimizing waste streams.

For illustration, the exploitation of high value low molecular weight compounds like phytosterols, namely β-sitosterol, lignans and triterpenoids from by-products of the industrial processing, like knots, bark or pulping liquors, is a strategy already implemented in some pulp industries [7].

Approximately 70 % of the pulp, based on eucalyptus (*Eucalyptus globulus*) with a small contribution of pine (*Pinus pinaster*), produced is exported, mainly to the European Union. *Eucalyptus* is used due to its higher productivity, lower rotation periods and long fibers allowing a higher quality of pulp and paper [8; 9]. According to preliminary results from IFN6, in 2010, eucalyptus was the specie that occupied the biggest area in Portugal, with 812 thousand hectares, followed by cork oak (*Quercus suber*) and

pine with 737 and 714 thousand hectares each [10]. This represents 3.2 million hectares, corresponding to 35.4 % of national territory. It has a 57 thousand hectares reduction since 2005. *Eucalyptus* species are the most important fiber sources for pulp and paper production in Portugal and Spain, where this sector has observed a fast growing during the last years. Several high-value triterpenic acids such as betulinic, betulonic, oleanolic and ursolic acids as well as the acetylated forms of the latter two were identified. Also, triterpenoids are the major constituents of the outer bark extractives obtained by Soxhlet dichloromethane extraction, making this part of the bark more interesting for an industrial valorization of this low-value stream from papermaking process [11; 12].

The main analytical methods for triterpenic acids are thin layer chromatography (TLC) [13], gas chromatography (GC) [14], high performance liquid chromatography (HPLC) coupled with ultraviolet (UV) [15] or with mass spectrometry (MS) [16], capillary zone electrophoresis (CZE) [17] and micellar electrokinetic chromatography (MEKC) [15]. However, due to the low volatility of triterpenic acids, derivatization steps are required for GC analysis. In the case of HPLC the detection requires wavelengths of approximately 200 nm due to low UV absorbance [18].

The main objective of this master thesis is studying the separation of two triterpenic acids (oleanolic and ursolic acids) from a mixture through chromatography, to perform their isolation by simulated moving bed (SMB) technology. This document is divided in 5 chapters. Chapter 1 is a introductory chapter which presents theoretical concepts for work comprehension. Chapter 2 describes the chromatographic system modeling for representing the breakthrough curve and simulate a SMB unit. Chapter 3 has the experiment procedures, materials and equipments used in the experiments. The results obtained are analyzed and discussed in Chapter 4, like the adequate mobile phase for separation and transport parameters determination. Chapter 5 gathers the principal conclusions of the work and some suggestions for future work.

1.1 Triterpenic acids

Triterpenic acids are high-value compounds that can be extracted from agricultural by-products prior to burning, while adding substantial economic value to biorefinery-based processes. Oleanolic acid (3β-hydroxy-olea-12-en-28-oic acid) and ursolic acid (3β-hydroxy-urs-12-en-28-oic acid) and their derivatives have been explored due to their nutraceutical and pharmacological proprieties, being widely used in agriculture, food and cosmetics industry.

Oleanolic acid, Figure 1.1 (a), is increasingly recognized for its wide range of important biological activities that provide beneficial health effects, including antidiabetic [15; 19; 20], antitumoral [21], antimicrobial [22], antioxidant [23], anti-inflammatory [16; 19; 20; 22; 23], hepatoprotective [15; 16; 18; 21], antiprotozoal [16; 22], cardiopro-

tective [19; 24] anti-ulcer [22] and neuroprotective effects [19; 24]. Oleanolic acid also revels anti-HIV and anti-allergic activities [6].

Ursolic acid , Figure 1.1 (b), has appreciable pharmacological effects including hepatoprotective [21], anti-inflammatory [16; 25], immunomodulatory [25; 26], antibacterial [27], antiviral [25], anti-angiogenesis [25; 28], antiproliferative [28], proapoptotic [28], antimetastatic [28], antioxidant effect [15; 28], antiulcer [19] and antidiabetic [19] activities. Recently, ursolic acid is an integral part of the human diet, implicated in protection and prevention against human cancers [16; 29; 30].

Oleanolic and ursolic acids are hydrophobic position isomers whose only difference is the configuration of methyl group. Although they are not chiral molecules, the hydrophobic cavities of cyclodextrins (CDs) can form inclusion complexes with the analytes, improving significantly the separation of components with distinct hydrophobic, isomers or chiral properties [15].

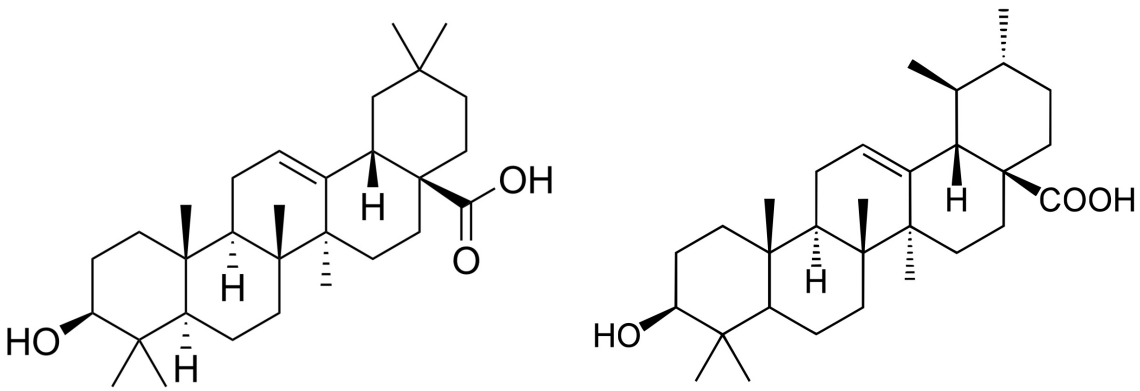

(a) Oleanolic acid (b) Ursolic acid

Figure 1.1: Chemical structures of triterpenic acids.

Oleanolic and ursolic acids can be isolated from various medicinal plants, leaves, flowers. Cuticular waxes are excellent sources of triterpenoids with a purpose in protection against biotic stresses (such as herbivores and pathogens) and on the mechanical properties of the fruit surface, which are partially responsible for allelopathic potential [26]. Forestry and agro-industrial wastes could be other sources, in general mainly concentrated in plants surface tissues like bark, stem or leaf and fruit waxes [6].

There are several extraction methods to recover triterpenic acids from diverse plant tissues involving the use of organic solvents of different polarities. The extracts are submit to clean-up or fractionation procedures for analytical purposes, such as simple preparative chromatography or solid phase extraction (SPE), with general or highly specific phases such as molecular imprinted polymers in order to obtain triterpenic acids enriched extracts or even pure compounds. The most usual approach for the analytical extraction of triterpenic acids is Soxhlet extraction with nonpolar solvents. Acceler-

ated solvent extraction (ASE), ultrasonic assisted extraction (UAE), microwave assisted extraction (MAE), supercritical fluid extraction (SFE) and ionic liquids extraction are alternatives to the conventional methods for their removal from diverse plant tissues [6].

Although the increasing number of studies and the interest for several industries for the beneficial proprieties of the acids and their applications in diverse areas, they are mainly produced for research purposes. Oleanolic and ursolic are sold by several chemical reagents providers, however, they are available in small quantities. Their prices oscillate, not having a reference value that permit a comparative analysis. Depending on their purity, oleanolic acid can reach 7800 €/g [31] and ursolic acid 21800 €/g [32].

1.2 Preparative chromatography

Chromatography is a simple, but crucial, separation process for isolation and purification of value added components from complex mixtures that is operated in the elution mode, where a mixture is injected at the inlet of a packed bed (adsorbent) through which flows a mobile phase (solvent). The principle of this process is based on the fact that different solutes have distinct affinities to the stationary phase so they travel with different velocities in the column. The less retained component will exit the column earlier than the more retained one, occurring the separation (Figure 1.2) [33],[34]. This was demonstrated by Don de Vault (Equation 2.8). This operation is not the most effective, especially for high quantities of mixture to be treated and difficult separations, due to low yields and high product dilution. [35].

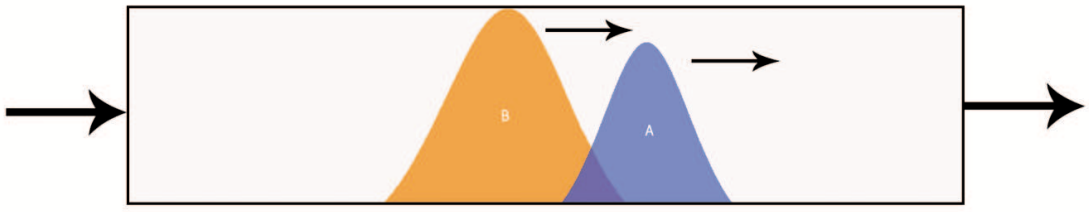

Figure 1.2: Preparative Chromatography scheme (Image adapted from [33]).

With a view to supply these limitations, True Moving Bed technology (represented in Figure 1.3.) introduced the movement of solid and liquid streams in countercurrent. Divided in four sections, the feed is continuously introduced in the middle of the system and two product lines are collected, one richer in the most retained compound called the extract (B), and the raffinate (A), which is richer in the less retained compound. The movement of both streams enables higher mass transfer driving force and, therefore higher productivity as opposed to other chromatographic techniques where one phase is usually stationary. The mechanical erosion of the adsorbent and wearing of the equipment are

the major problems of this mechanism, which may turn in high maintenance costs [36].

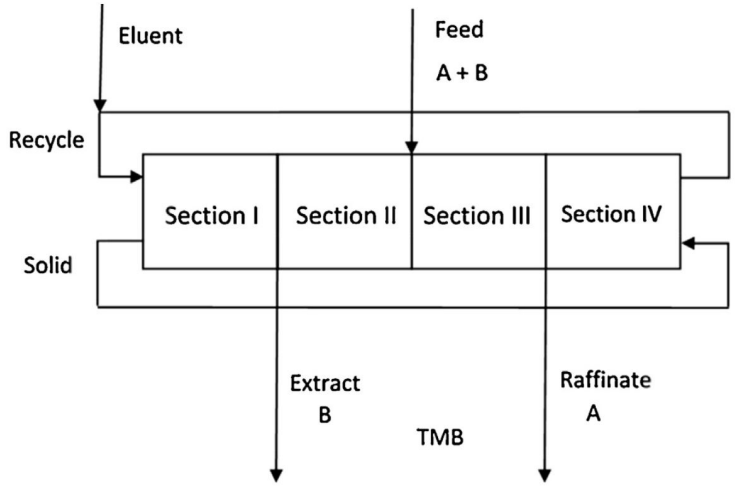

Figure 1.3: Schematic representation of True Moving Bed mechanism [37].

1.3 Simulated Moving Bed (SMB) and SMB modifications

Simulated Moving Bed (SMB) is a continuous chromatographic technique, which eliminates drawback of batch chromatography, where high resolution is a crucial parameter, by only requiring low resolutions. The operation involves countercurrent movement of a liquid eluent phase and a solid adsorbent phase simulated by periodically shifting columns with a rotary valve allowing a continuous operation to increase productivity and save fresh solvent, consequently resulting in an economically viable process. This separation technology has establish several applications in diverse areas such as sugar, petrochemical, fine chemical and chiral separations [38].

In Figure 1.4., a schematic representation of a SMB unit is shown. There are four sections, two inlet streams (feed and eluent) and two outlet streams (raffinate and extract).

The four sections are delimited by the position of the external streams in each cycle and have different roles: In Section I occurs the regeneration of the adsorbent; in Section II the less retained component (A) is desorbed; in Section III the more retained component (B) is adsorbed, and the eluent is regenerated in Section IV.

The switch time interval (t^*) is crucial and must be specifically tailored for obtaining high purity and productivity [36].

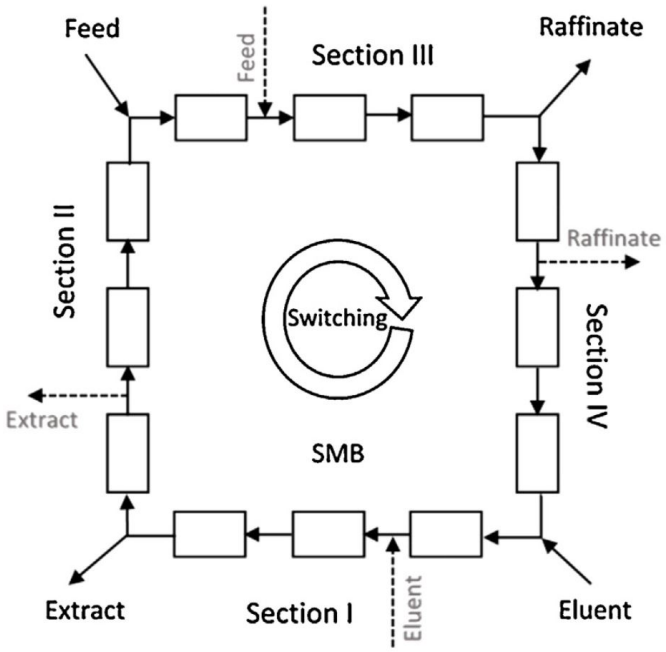

Figure 1.4: Schematic representation of Simulated Moving Bed mechanism [37].

SMB was developed by Universal Oil Products (UOP) in 1961 and has been used in the chemical industry for several separations known as Sorbex processes. This process include the Molex, commercialized in 1964 for extraction of paraffins from branched and cyclic hydrocarbons, the Parex process (1971) for separation of p-xylene from a mixture of C8 aromatics, the Olex to separate olefins from paraffins, and the Sarex for sugar purification [39].

SMB applications have shifted mainly to the fine chemistry and pharmaceutical industries. Separations of enantiomers have been performed with great success via SMB process granting the development of enantiomeric pure substances in opposition to a racemic mixture that could not be desirable [34]. In the last years, the interest caused by the success of this technology in several areas lead to many modification technologies of the conventional SMB chromatography, increasing the efficiency of existing processes and allowing to accomplish separations that would otherwise be impossible [40]. This can be verified by the emerging of the number of scientific articles of the various SMB operation modes, represented in Figure 1.5.

They are classified by considering the major modifications like dynamic configurations (Varicol and PseudoSMB), modulation of the flow rate (PowerFeed, Outlet Swing Stream), concentration modulation (ModiCon, Enriched Extract SMB), gradient operation (Solvent Gradient, Temperature Gradient). Multi-component separation like ternary separation was also accomplished by SMB process with three-zone or five-zone arrangements, the cascades of SMB process, and the JO process (PseudoSMB). To these uncon-

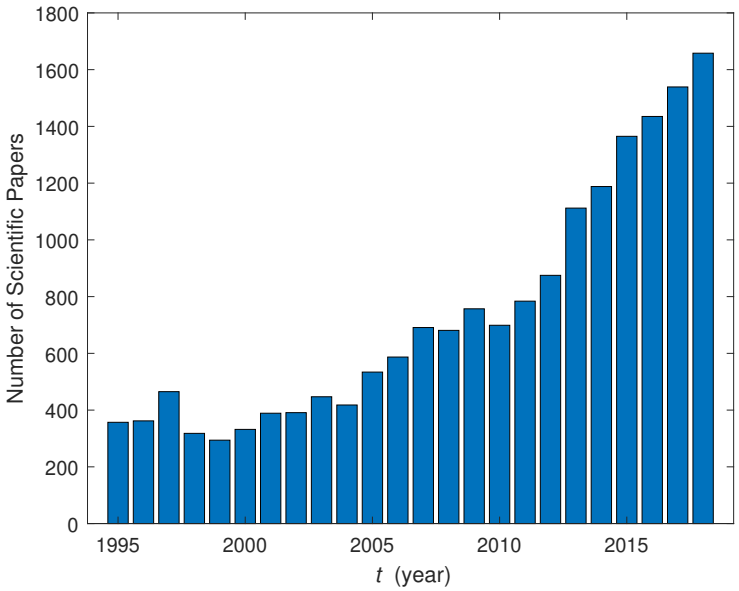

Figure 1.5: Evolution of the number of scientific papers with "Simulated Moving Bed" keywords, over time, since 1995 [41].

ventional operating modes are associated numerous advantages and limitations [40].

PowerFeed

Also called time variable SMB, all the flow rates in this process vary during switching intervals. It works by dividing each switch time interval in subintervals in which different flow rate values are applied. This process has shown to allow the reduction of solvent consumption and increased productivity in contrast to the traditional SMB [34].

Varicol

Novasep Company (France) proposed the Varicol process (Figure 1.6), patented in 2000. It is characterized by the asynchronous shifting for the positions of the inlet and outlet lines. The number of columns in each zone is different within the switch time, while the number of columns in each zone is constant for SMB process with the synchronous shifting. This makes the process more powerful than conventional SMB, namely higher productivity for the same purity [36].

ModiCon process

This process is a variation of the SMB where the feed concentration is modulated within the switch time, divided into several sub-intervals. This process exploits the fact that the propagation velocities of the components in non-linear chromatography are

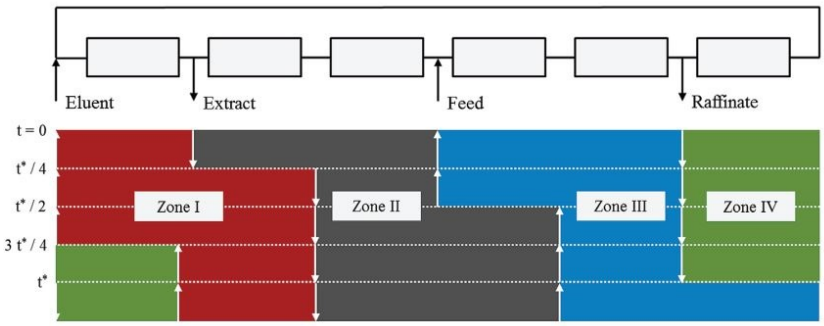

Figure 1.6: Scheme of a 6 column Varicol configuration: switching of the lines over a period [34].

concentration dependent and tries to optimize performance, tuning them. The major advantages are related with its ability to provide the target product with an increased purity value [33].

Gradient SMB - Solvent and Temperature

When applying a solvent gradient, achieved by modifying the concentration of the strongest component of the solvent mixture allows a higher separation resolution and a reduction in eluent consumption is called Solvent Gradient SMB (SG SMB). This method was successfully applied to systems for which the adsorption equilibrium is strongly dependent on the solvent composition, nevertheless, attention must be drawn to the solubility of the solute over the entire range of solvent compositions within the unit.

When manipulating temperature in an SMB system to modify adsorption behavior in each section and thus improve the separation performance, this is called Temperature Gradient SMB operation (TG SMB). TG SMB can be interesting in SMB reactors where temperature variations can be used to influence both adsorption and reaction kinetics. [40].

PseudoSMB

Described as "JO chromatographic separation device", applied by Japan Organo company, PseudoSMB is a cyclic process used for ternary mixtures, which consists in the following two steps, represented in Figure 1.7:

Step 1 - The feed and desorbent enter the system, operated to equivalent to a series of chromatographic columns. The target component of intermediate adsorption strength is collected.

Step 2 - There is only one inlet flow of eluent and no feed, the more retained recovered in the extract and the less adsorbed specie is collected in the raffinate [42], [43].

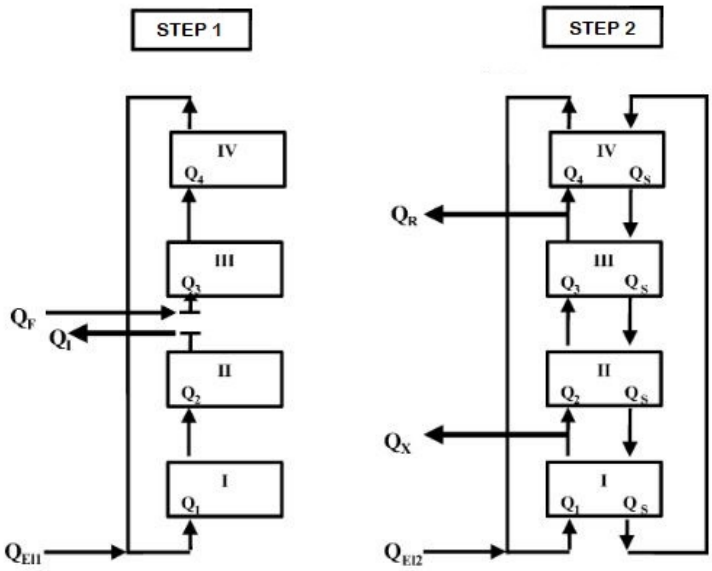

Figure 1.7: Representation of PseudoSMB device (Image adapted from [35]).

Outlet Swing Stream

Outlet Swing Stream, Figure 1.8, is a complex modulation of SMB outlet streams flow rate. The flow rates in sections IV and I are dynamically adjusted, keeping a constant value in other two sections (II and III), through the manipulation of the extract, raffinate and eluent flow rates. Hence, the expansion or contraction of the ports of product concentration fronts can increase the purity of the target species or decreasing the eluent consumption [34].

Supercritical SMB (SF SMB)

The main characteristic of SF SMB, represented in Figure 1.9, is the possibility of tuning the elution strength of the mobile phase in the different zones of the SMB unit, to optimize its separation performance. Has as advantages the using of supercritical fluids that reduces significantly the consumption of organic solvents and the environmental problems associated with them.

Physicochemical properties of supercritical fluids like viscosity and diffusivity are favorable in comparison of those of liquids and the retention behavior of solutes in supercritical fluid chromatography demonstrates a strong dependence on mobile phase density, which could be tuned in order to increase the performance of the process [44].

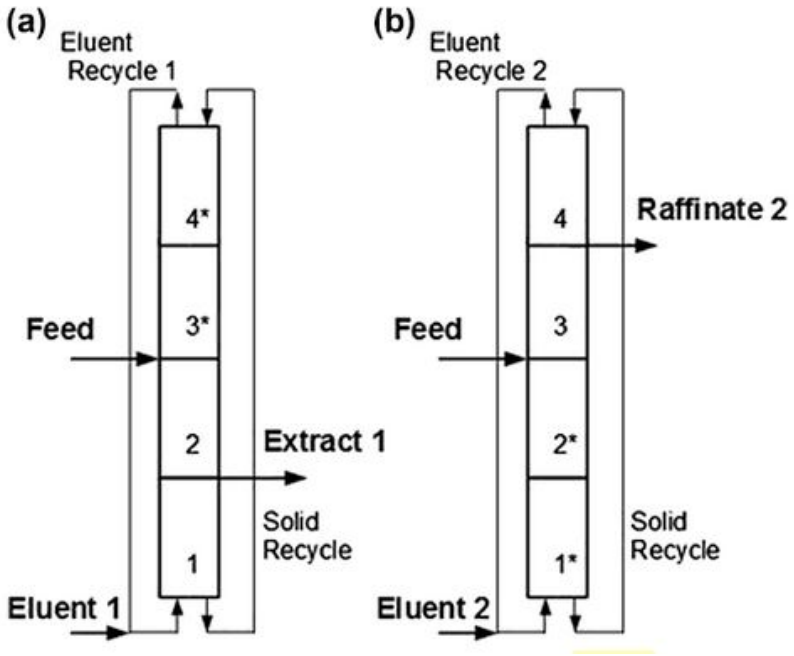

Figure 1.8: Schematic representation of Outlet Swing Stream process [35].

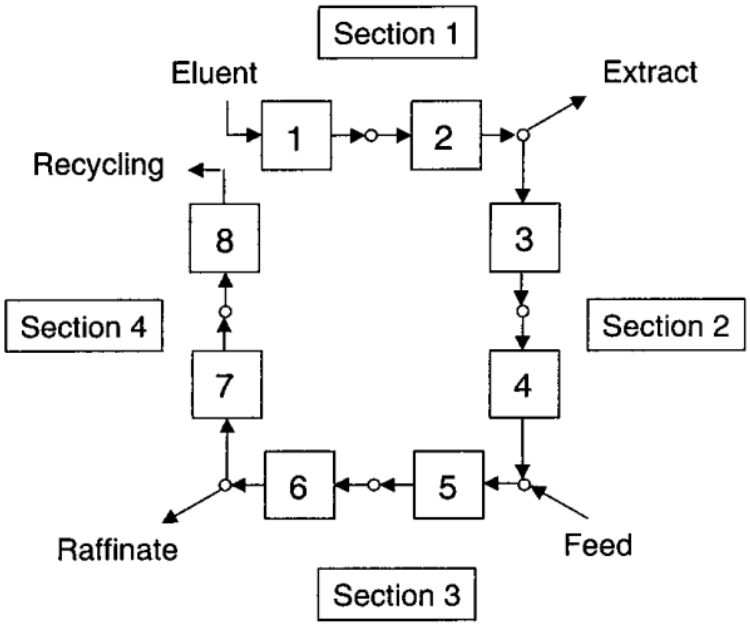

Figure 1.9: Scheme of a SF SMB unit with four sections [45].

Intermittent SMB (I SMB)

This process, represented in Figure 1.10, is similar to the conventional SMB process. However, the switch period is divided into two substeps:

In the first one, the unit is operated as a SMB without flow in section 4;

In the second substep all inlet and outlet ports are closed, where the fluid circulates through the column train to adjust the relative position of the concentration profiles. [46].

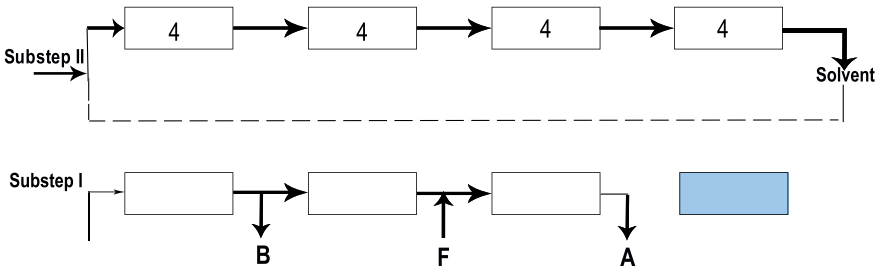

Figure 1.10: Schematic representation of Intermittent-SMB mechanism (Image adapted from [46])(A - Less retained component, B - more retained component and F - Feed).

SMB cascades

The simpler case of this technology is the separation of a ternary mixture using two consecutive SMB units: in the first unit, either the more or the least retained species is separated from the components present in the feed stream. The resulting binary mixture is introduced in the second unit and then the separation process is completed. SMB cascades allow to independently adjust all process parameters associated with the studied chromatographic separation, as the switching time, temperature or stationary phase used in each unit, in order to achieve superior performances. However, the high desorbent amounts required to elute the target species establish an elevated dilution factor in the outlet streams, those increments after every additional separation step, leading to reduced productivity values [40]. In Figure 1.11 is represented a scheme with SMB cascades.

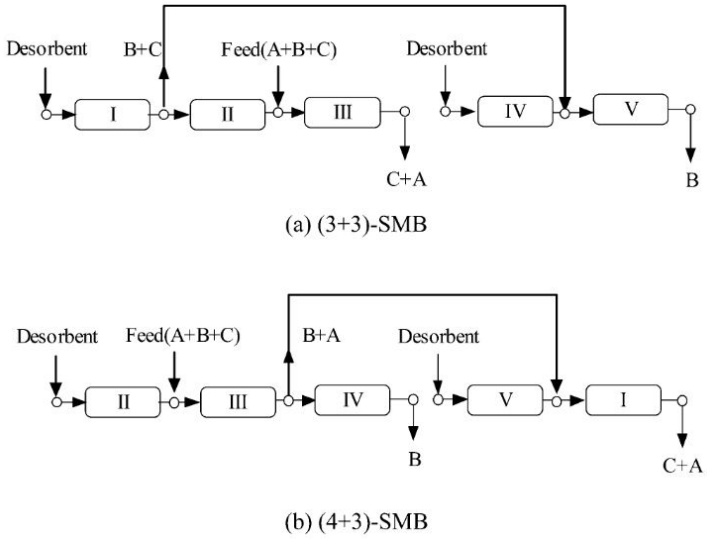

Figure 1.11: SMB cascades schemes. (a) represents a (3+3)-SMB which is composed by two 3-zone SMBs that share zone III and (b) a (4+3)-SMB is shown, composed by a 4-zone and a 3-zone SMB that share zones I and IV. A, B, and C represent the least, the intermediate, and the most retained solute, respectively [47].)

2 Modeling

2.1 Adsorption Isotherms

Modeling an adsorption isotherm is crucial for predicting the chromatographic separation. Linear models are generally valid for analytical chromatography, which operates with low concentrations. The mathematical expression of linear isotherm is:

$$q_i = H_i C_i \tag{2.1}$$

where q_i is the solid phase concentration, H_i is the equilibrium constant and C_i is the liquid phase concentration.

In preparative chromatography, operating conditions allows working in a wide range of high concentrations and in such conditions usually appear deviations to the linear model that lead to competition between different compounds [34].

Langmuir is the most common isotherm in preparative chromatography. Considers that the adsorbent surface is homogeneous and each active site adsorbs one solute molecule, having only one layer and there are have not interactions between adsorbed molecules [48].

For binary mixtures, the Langmuir isotherm is given by:

$$q_i = \frac{Q b_i C_i}{1 + b_1 C_1 + b_2 C_2} \tag{2.2}$$

where parameter Q corresponds to adsorbent capacity, and b_1 and b_2 represent the equilibrium constants of the the less and more retained compounds.

Combining Equation (2.1) with (2.2) results:

$$q_i = H_i C_i + \frac{Q b_i C_i}{1 + b_1 C_1 + b_2 C_2} \tag{2.3}$$

This model considers that the adsorbent has selective sites, described by the Langmuir contribution, and non-selective places, represented by H_i, [34].

Other complex models can also be use, like Bi-Langmuir Isotherm, which contains

two competitive Langmuir terms:

$$q_i = \frac{Qb_i C_i}{1 + b_1 C_1 + b_2 C_2} + \frac{Qb'_i C_i}{1 + b'_1 C_1 + b'_2 C_2} \tag{2.4}$$

Langmuir-Freundlich isotherm is another model used for binary mixtures, represented by:

$$q_i = \frac{Qb_i C_i^{n_i}}{1 + b_1 C_1^{n_1} + b_2 C_2^{n_2}} \tag{2.5}$$

if n_1=n_2=1, Equation 2.5 results in Equation 2.2.

2.2 Equilibrium model for adsorption column

The material balance for compound i in an adsorption column is crucial for the knowledge of column dynamics. The elementary case represents the ideal adsorption column which considers plug flow in column, instantaneous equilibrium between the fluid and solid in every point of the column, and negligible mass transfer resistances.

$$u_i \frac{\partial C_i}{\partial z} + \frac{\partial C_i}{\partial t} + \frac{1 - \varepsilon_b}{\varepsilon_b} \frac{\partial q_i^*}{\partial t} = 0 \tag{2.6}$$

where u_i is linear velocity, ε_b is bed porosity and q^* is solid phase concentration in equilibrium with liquid phase. Combining with the adsorption equilibrium isotherm:

$$q_i^* = f(C_i) \tag{2.7}$$

it can be demonstrated, applying the cyclic relation between partial derivatives, that the velocity of propagation of a concentration C_i is:

$$u_{Ci} = (\frac{dz}{dt})_{C\mathrm{i}} = \frac{u_i}{1 + (\frac{1-\varepsilon_b}{\varepsilon_b}) f'(C_i)} \tag{2.8}$$

where z is the axial position, t corresponds to time, $u_{C\mathrm{i}}$ is velocity of propagation of a concentration i and f'(C_i) is the slope of the isotherm relating the adsorbed phase concentration ${q_\mathrm{i}}^*$ in equilibrium with C_i [35].

Don de Vault extracted the principle basics for percolation. The equilibrium theory indicates that, for favorable isotherms, the concentration front in the adsorption step is compressive, so higher concentrations travel at higher velocities, with a shock as limit (Figure 2.1 (a)). For unfavorable isotherms, the concentration front is dispersive because higher concentrations travel at lower velocities (Figure 2.1 (c)) [34].

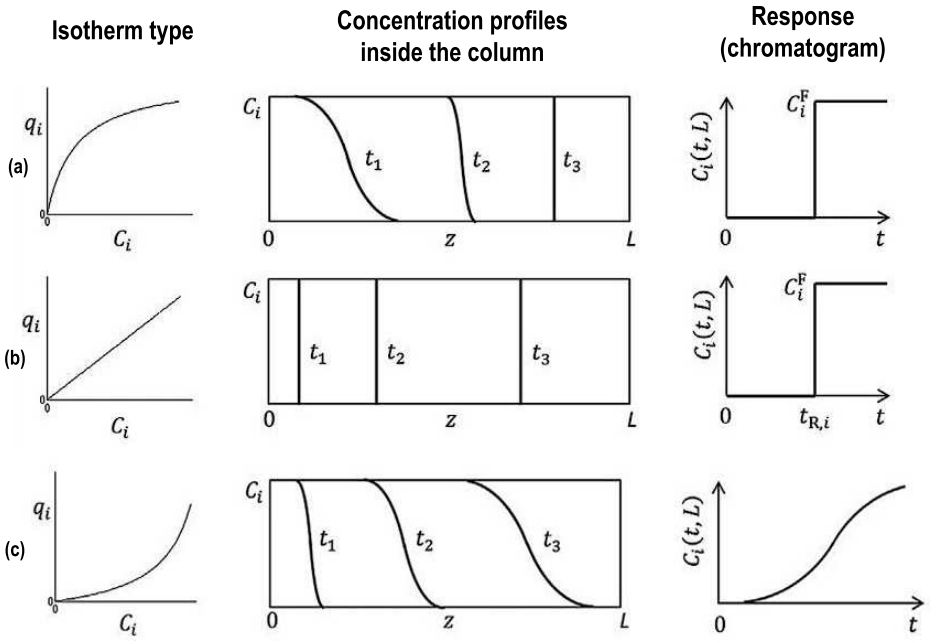

Figure 2.1: Schematic diagram of concentration profiles inside the column and system responses in the cases of favorable, linear and unfavorable isotherms, respectively (Image adapted from [34]).

2.3 Real adsorption column

Adsorption in real columns depends on various factors, like hydrodynamics, axial dispersion, mass transfer kinetics and adsorption isotherms.

Assuming plug flow with axial dispersion (D_{ax}), the material balance for compound i in a column volume is:

$$-D_{ax}\frac{\partial^2 C_{ib}}{\partial z^2}+u_i\frac{\partial C_{ib}}{\partial z}+\frac{\partial C_{ib}}{\partial t}+\frac{1-\varepsilon_b}{\varepsilon_b}\frac{\overline{\partial q}}{\partial t}=0 \tag{2.9}$$

Furthermore, the material balance for compound i in adsorbed phase is given by:

$$\frac{\partial q_i}{\partial t}=\frac{D_{eff}}{r^2}\frac{\partial}{\partial r}(r^2\frac{\partial q_i}{\partial r}) \tag{2.10}$$

where D_{eff} is effective diffusion coefficient and $\overline{q}$ is average concentration in the solid phase and it is given by:

$$\overline{q_i}=\frac{3}{R^3}\int_0^R r^2 q_i dR \tag{2.11}$$

The initial conditions are

$$t=0 \quad (\forall\ z), \quad C_{ib}=0 \tag{2.12}$$

$$t=0 \quad (\forall\ r), \quad q_i=0 \tag{2.13}$$

and the boundary conditions are

$$z = 0 \ (\forall t \geqslant 0), C_{ib} = C_{iF} + \frac{D_{ax}}{u_i}\frac{\partial C_i}{\partial z} \tag{2.14}$$

$$z = L, \frac{\partial C_{ib}}{\partial z} = 0 \tag{2.15}$$

$$r = 0, \frac{\partial q_i}{\partial r} = 0 \tag{2.16}$$

$$r = R, q_i = q_{i,s} \tag{2.17}$$

Assuming the linear driving force model (LDF) for mass transfer, the solute i accumulation in solid is given by:

$$\frac{\partial \overline{q_i}}{\partial t} = K_{LDF,i}(q_i^* - \overline{q_i}) = K_{LDF,i}H_i(C_{ib} - C_i^*) \tag{2.18}$$

where $K_{\mathrm{LDF,i}}$ is the LDF global coefficient of mass transfer of component i, H_{i} is equilibrium constant of adsorption (q_{i}=$H_{\mathrm{i}}C_{\mathrm{i}}$) and $C_{\mathrm{i}}{}^*$ is equilibrium concentration with $\overline{q_i}$.

When the isotherm is linear, LDF model is applicable, axial dispersion is neglactable and the fluid velocity is uniform, the equations that models the adsorption process in fixed bed has an analytical solution given by Anzelius.

Klinkenberg improved the following useful approximation that adjusts very well the analytical solution of Anzelius, with an average error of < 0.6 % , for φ>2 [49]:

$$\frac{C_i}{C_{iF}} \approx \frac{1}{2}[1 + erf(\tau - \varphi + \frac{1}{8\sqrt{\tau}} + \frac{1}{8\sqrt{\varphi}})] \tag{2.19}$$

where error function is represented by

$$erf(x) = \frac{2}{\sqrt{\pi}}\int_0^x \exp(-x^2)dx \tag{2.20}$$

and φ and τ are dimensionless distance and displacement-corrected time coordinates, respectively, given by:

$$\varphi = \frac{H_i K_{LDF,i}}{u_i}(\frac{1-\varepsilon_b}{\varepsilon_b})z \tag{2.21}$$

$$\tau = K_{LDF,i}(t - \frac{z}{u_i}) \tag{2.22}$$

2.4 SMB modeling

The modeling of a SMB unit it can be performed by two different strategies: one, by simulating the SMB system directly, considering periodic movement of inlet and outlet

streams of the unit, with a stationary solid phase; and other, by representing its operation equivalent to a true moving bed (TMB) unit, in which the both solid and liquid are in countercurrent [35].

SMB considers that solid is fixed in columns, but the movement is simulated by periodic change of the inlets and outlets of SMB unit. Plug flow with axial dispersion is used frequently to describe the fluid phase flow.

Since each column plays a different role depending on the section it belongs, the boundary conditions for each column change after each switch time. Therefore, a cyclic steady state (CSS) is reached in a SMB, instead of a real steady state that happens in the TMB operation. Once CSS is achieved, the internal concentration profile is variable through one cycle, however it is identical in the same instance of time in consecutive cycles. TMB assumes that solid and liquid move in opposite directions [50].

Considering that inlet and outlet are fixed, the interstitial velocity of liquid in SMB unit is the sum of interstitial velocities of liquid and solid in TMB and it is given by:

$$v_j^* = v_j + u_s; \quad u_s = \frac{L_c}{t^*} \tag{2.23}$$

where the v_{j} and v_{j}^* are interstitial liquid velocity in section j of the SMB and TMB and u_{s} is interstitial solid velocity. t^* is the switching time in SMB model and is related to u_{s} and L_{c}.

Predicting the SMB unit performance by equivalent TMB model is more precise when bigger is the number of columns per section. The design of a TMB unit consists in defining the flow rate in each section ensuring the desirable separation [51].

The material balance for compound i in a column j can be expressed as:

$$\frac{\partial C_{ib}}{\partial t} = D_{ax,ij}\frac{\partial^2 C_{ib}}{\partial z^2} - v_j^*\frac{\partial C_{ij}}{\partial z} - \frac{(1-\varepsilon)}{\varepsilon}\frac{\partial \overline{q_{ij}}}{\partial t} \tag{2.24}$$

which $D_{\mathrm{ax,ij}}$ represents axial dispersion, $C_{\mathrm{i,j}}$ is the concentration of the solute in the fluid. z is the axial coordinate and t corresponds to time.

In addition the material balance of compound i in adsorbed phase of column is given by:

$$\frac{\partial \overline{q_{ij}}}{\partial t} = K_{LDF,ij}(q_{ij}^* - \overline{q_{ij}}) \tag{2.25}$$

where $K_{\mathrm{LDF,ij}}$ is the global LDF mass transfer coefficient, q_{ij}^* is the solid phase concentration in equilibrium with the fluid phase and $\overline{q}$ is the average concentration in the solid.

Considering the isotherm, in which :

$$q_{ij}^* = H_i C_{ij} \tag{2.26}$$

Initial conditions (t=0)

$$C_{ij}^{n=0} = 0 \quad or \quad C_{ij}^{n+1} = C_{ij}^{n} \tag{2.27}$$

$$q_{ij}^{n=0} = 0 \quad or \quad \overline{q_{ij}}^{n+1} = \overline{q_{ij}}^{n} \tag{2.28}$$

Boundary condition (z=0)

$$C_{ij} = -\frac{Dax_{ij}}{v_j}\frac{\partial C_{ij}}{\partial z} = C_{ij,0} \tag{2.29}$$

where $C_{\mathrm{ij,0}}$ is the inlet concentration for specie i [35].

Bondary condition (z=L)

For column inside a section, and for raffinate and extract nodes:

$$C_{ij} = C_{ij+1.0} \tag{2.30}$$

Eluent node:

$$C_{ij} = \frac{v_I^*}{v_{IV}^*} C_{ij+1.0} \tag{2.31}$$

Feed node:

$$C_{ij} = \frac{v_{III}^*}{v_{IV}^*} C_{ij+1.0} - \frac{v_F}{v_{II}^*} C_i^F \tag{2.32}$$

The global balances to the nodes between each section relating the internal and velocities of the feed, raffinate, eluent and extract are:

Eluent node:

$$v_I^* = v_{IV}^* + v_E \tag{2.33}$$

Extract node:

$$v_{II}^* = v_I^* - v_x \tag{2.34}$$

Feed node:

$$v_{III}^* = v_{II}^* + v_F \tag{2.35}$$

Raffinate node:

$$v_{IV}^* = v_{III}^* + v_R \tag{2.36}$$

Some restrictions are defined, allowing the possibility of recovering the less retained compound (A) from raffinate stream and the more retained compound (B) from extract. These restrictions can be expressed in terms of the net fluxes of each component in each

section [51]:

$$\frac{Q_I C_{B,I}}{Q_S q_{B,I}} > 1;\ \frac{Q_{II} C_{A,II}}{Q_S q_{A,I}} > 1 \ \ and \ \ \frac{Q_{II} C_{B,II}}{Q_S q_{B,II}} < 1 \tag{2.37a}$$

$$\frac{Q_{III} C_{A,III}}{Q_S q_{A,III}} > 1 \ \ and \ \ \frac{Q_{III} C_{B,III}}{Q_S q_{B,III}} < 1;\ \frac{Q_{IV} C_{A,IV}}{Q_S q_{A,IV}} < 1 \tag{2.37b}$$

where Q_{j} is the volumetric liquid flow rates in section j of the TMB, Q_{S} is the solid flow rate and $q_{\mathrm{B,j}}$, $q_{\mathrm{A,j}}$ are the adsorbed concentrations of more and less retained species each in section j.

In a binary system context with a linear adsorption isotherms, assuming that occurs instantaneous equilibrium, simple formulas can be derived to evaluate the better TMB flow rates. In the linear case, the net flux constrains presented in Equations 2.36 are reduced to four, that are [35]:

$$\frac{Q_{\mathrm{I}}}{Q_{\mathrm{S}}} > H_{\mathrm{B}} \tag{2.38a}$$

$$\frac{Q_{\mathrm{II}}}{Q_{\mathrm{S}}} < H_{\mathrm{B}} \ \ and \ \ \frac{Q_{\mathrm{II}}}{Q_{\mathrm{S}}} > H_{\mathrm{A}} \tag{2.38b}$$

$$\frac{Q_{\mathrm{III}}}{Q_{\mathrm{S}}} > H_{\mathrm{B}} \ \ and \ \ \frac{Q_{\mathrm{II}}}{Q_{\mathrm{S}}} < H_{\mathrm{A}} \tag{2.38c}$$

$$\frac{Q_{\mathrm{IV}}}{Q_{\mathrm{S}}} < H_{\mathrm{A}} \tag{2.38d}$$

where H_{B} and H_{A} are the more retained and less retained species linear coefficients, respectively.

Assuming that all these inequalities are satisfied by the margin β>1, Equations 2.37 can be rewritten as:

$$\frac{Q_I}{Q_S H_B} = \beta \tag{2.39a}$$

$$\frac{Q_{II}}{Q_S H_A} = \beta \tag{2.39b}$$

$$\frac{Q_{III}}{Q_S H_B} = \frac{1}{\beta} \tag{2.39c}$$

$$\frac{Q_{IV}}{Q_S H_A} = \frac{1}{\beta} \tag{2.39d}$$

noticing that

$$Q_E = Q_I - Q_{IV};\ Q_X = Q_I - Q_{II};\ Q_F = Q_{III} - Q_{II};\ Q_R = Q_{III} - Q_{IV} \tag{2.40}$$

where Q_{E}, Q_{X}, Q_{F} and Q_{R} are the eluent, extract, feed and raffinate volumetric flow rates, respectively. Hence, the restriction of the β parameter and the solid flow rate (or, in alternative, one of the liquid flow rate) defines all the flow rates throughout the TMB

system. It should be mention that the β parameter also has a higher limit. The feed flow rate must be higher than zero [35]. The interval of possible values for the β parameter is [52]:

$$1 < \beta < \sqrt{\frac{H_B}{H_A}} \tag{2.41}$$

The limiting case of β=1 is equivalent to the situation in which dilution of species is minimal, and the extract and raffinate product concentrations approach the feed concentrations [35]. For β>1 we have: $Q_{\mathrm{I}} > Q_{\mathrm{III}} > Q_{\mathrm{II}} > Q_{\mathrm{IV}}$.

Considering a situation of complete separation, it follows that the concentration of the less retained component in the raffinate and the more retained component in the extract obtained are [50]:

$$C_A^R = \frac{Q_F}{Q_R} C_A^F \tag{2.42a}$$

$$C_B^R = \frac{Q_F}{Q_X} C_B^F \tag{2.42b}$$

In conclusion, the raffinate and extract concentrations in the TMB operation under linear conditions will never exceed the feed concentrations. The volumetric flow rate in the SMB unit can be determined by equivalencing SMB and TMB.

$$Q_j^* = Q_j + \frac{\varepsilon_b}{1-\varepsilon_b} Q_S \tag{2.43}$$

Triangle theory

Triangle theory is a very useful design methodology that allows easy estimation of the boundaries of separation region, in order to achieve a complete separation of two compounds. Neglecting axial dispersion and mass transfer resistances, the conditions based on the equilibrium theory are set as in an ideal system [53].

Frequently, to represent the fluid and solid flow rates is used the following ratio $\mathrm{m_j}$:

$$m_j = \frac{Q_j^* t^* - \varepsilon_b V_c}{V_c(1-\varepsilon_b)}, \quad j \equiv I, II, III, IV \tag{2.44}$$

The operating conditions are determined according to m_{II} and m_{III} and triangle vertex provides the optimal operating condition for the ideal system. For linear adsorption isotherm, the triangle becomes rectangular (Figure 2.2).

In linear isotherm case, the restrictions for complete separation are:

$$m_{I,min} \leq m_I \tag{2.45a}$$

$$m_{II,min} \leq m_{II} \leq m_{II,max} \tag{2.45b}$$

$$m_{III,min} \leq m_{III} \leq m_{III,max} \tag{2.45c}$$

$$m_{IV} \leq m_{IV,max} \tag{2.45d}$$

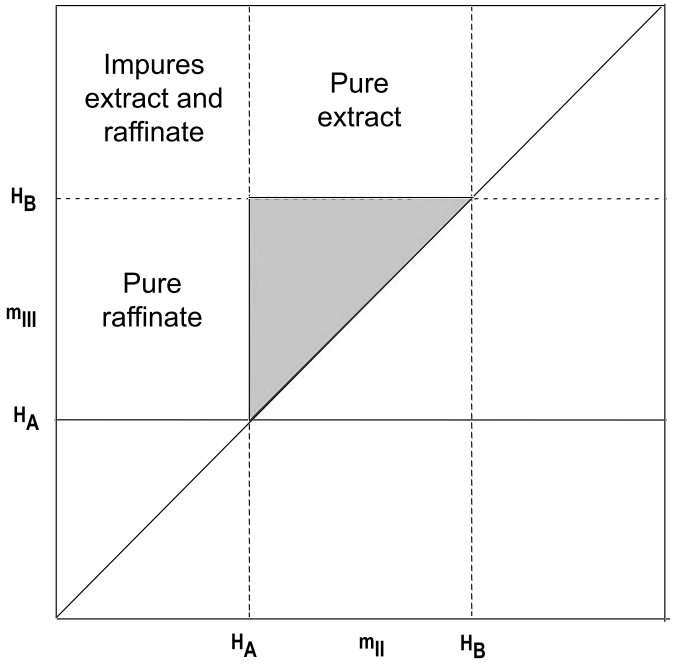

Figure 2.2: Separation zone of species with linear adsorption isotherm, the grey area corresponds to the pure extract and raffinate zone (adapted from [33]).

Performance criteria

The evaluation of SMB performance is based on the parameters: purity of products, solutes recovery, solvent consumption, and productivity [50].

Extract and raffinate purities (PuX and PuR) characterize the ratio between concentration of desired component and the total concentration of all solutes [50].

$$PuX = \frac{C_B^X}{C_A^X + C_B^X} \times 100 \tag{2.46a}$$

$$PuR = \frac{C_A^R}{C_A^R + C_B^R} \times 100 \tag{2.46b}$$

Extract and raffinate recoveries ($RecX$ and $RecR$) represent the ratio between the amount of a particular specie in the corresponding product stream within a switching period and the total amount of that species fed [33].

$$RecX = \frac{Q_X C_B^X}{Q_F C_B^F} \times 100 \tag{2.47a}$$

$$RecR = \frac{Q_R C_A^R}{Q_F C_A^F} \times 100 \tag{2.47b}$$

Solvent Consumption (SC) is the total volume of solvent used per unit mass of the solutes in feed [50].

$$SC = \frac{Q_E + Q_F}{Q_F(C_A^F + C_B^F)} \tag{2.48}$$

Productivity ($Prod$) is the amount of racemic mixture processed per unit volume of stationary phase and per unit time [50].

$$Prod = \frac{Q_F(C_A^F + C_B^F)}{V_T} \tag{2.49}$$

3 Experimental section

In this section are presented the materials and equipments for the execution of laboratory experiments and their procedures.

The objective is to study adequate solvents for the separation of triterpenic acids (oleanolic and ursolic acids) through preparative high performance liquid chromatography (HPLC). For mobile phase selection, factors like selectivity, resolution, solubility of solute and viscosity are fundamental.

3.1 Reagents

The analytical standards of oleanolic and ursolic acids were supplied from Aktin Chemicals for the chromatographic assays, and while for the breakthrough experiments oleanolic and ursolic acids from AK Scientific were used. The solvents methanol, water, ethanol, 2-propanol, 1-butanol, acetonitrile were supplied from Sigma Aldrich, and acetic acid was supplied from VWR.

3.2 Solubility measurement

In order to measure the solubility of triterpenic acids, a analogous procedure to the gravimetric method proposed by Gracin and Rasmuson was carried out [54]. For that, an excess of each acid was introduced in volumetric flasks that already contained solvent (Methanol/Water 95/5 (% v/v)) for a good detection of the two phases. The solution was filtered with a membrane and small amounts of solution (2, 3 and 5 mL) were transfered to previously weighed glass vials. It is important to refer that the filter is chemically compatible with the solvent. Finally, the vials were introduced in an oven at 45 °C until the solvent evaporated. Then the vial with residue (W_{VR}) was weighted. The solubility of acids in Methanol/Water 95/5 (%, v/v) was calculated by:

$$S = \frac{(W_{VR} - W_V}{V_S} \times 10^3 \tag{3.1}$$

where S is the solubility of the triterpenic acid, W_{V} is the previously weighed glass vial mass, W_{VR} is the mass of the glass vial and the residue. S is expressed in mass (g) of

solute per unit volume of solvent, V_S (mL).

3.3 Equipment

The chromatographic studies were conducted in a HPLC (High Performance Liquid Chromatography) equipment Gilson (Figure 3.1), which has two pumps (805 manometric module and 306 gradient), a mixture camera (811C dynamic mixer) and an UV-Vis detector (118 UV-Vis). The Unipoint Gilson software (version 5.11), presented in Figure 3.2, gives the data acquisition. The Acclaim C30 was the analytical column used (5 μm, 4.6 x 250 mm) which is filled with triacontyl silica (C30).

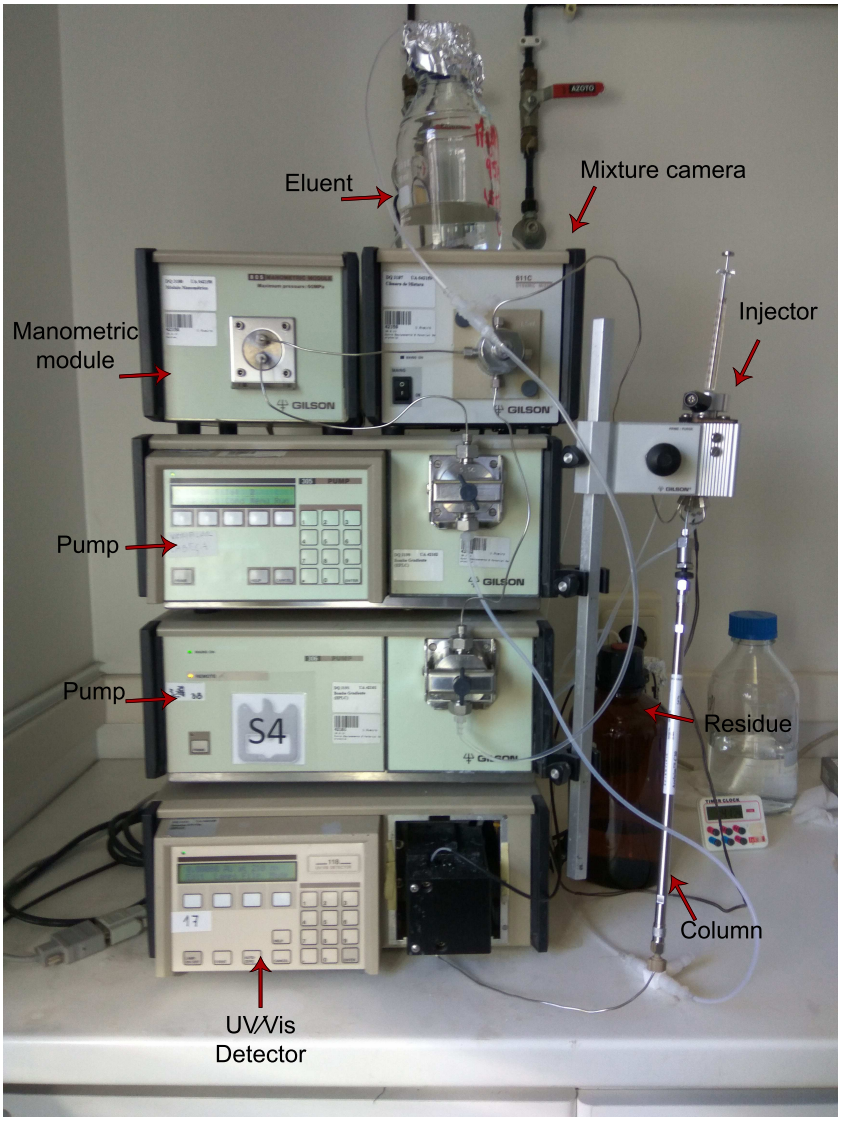

Figure 3.1: HPLC equipament used to study the separation of triterpenic acids.

3.4 Chromatographic pulse experiments

With the objective of selecting the most appropriate solvent or solvent mixture for the separation of oleanolic and ursolic acids, the following mobile phases were tested: Methanol 100 %, methanol/water 95/5 %, methanol/water 90/10 %, acetonitrile/methanol 70/30 %, methanol/acetonitrile 80/20 %, methanol/n-butanol 80/20 %, methanol/water 95/5 % + 500 μL acetic acid, methanol/water 90/10 % + 500 μL acetic acid, methanol/2-propanol 80/20 % and ethanol 100 %. All mobile phases are in % v/v. As has been referred above, an Acclaim C30 column was used in all assays.

3.4.1 Solution preparation for injections

It were prepared solutions, in 20 mL volumetric flasks, of OA and UA in methanol. The concentrations of the solutions were $C_{\mathrm{OA}} = 0.600$ mg/mL and $C_{\mathrm{UA}} = 0.895$ mg/mL.

3.4.2 Experimental procedure

The chromatography experiments were carried out in a HPLC equipment Gilson by introducing several pulses of TTAs solutions (oleanolic acid + ursolic acid) into the various mobile phases. The experimental procedure was the following one:

1. Insert the admission tube, with the filter in the extremity, inside the mobile phase recipient;
2. Turn on the equipment and the computer for the data acquisition;
3. Open the Unipoint Gilson Software (Figure 3.2);
4. Set the flow rate and wavelength suitable for the experiment;
5. Make the mobile phase flow through the column and purge the system;
6. Proceed with the system stabilization with mobile phase;
7. Inject the sample in the column;
8. Press START;
9. After the complete visualization of the chromatographic peaks in the computer, press STOP button;
10. Save the chromatogram.

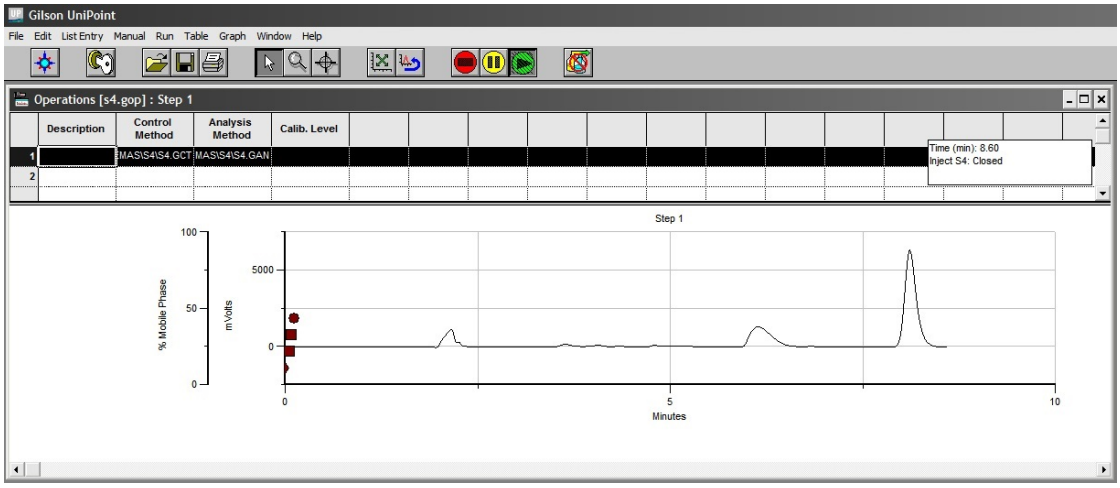

Figure 3.2: Gilson UniPoint software (Version 5.11) (Gilson, Inc., Middleton, WI,USA) used for collecting data from HPLC.

3.4.3 Operating conditions

The operating conditions of each experiment are represented in Table 3.1: mobile phase, flow rate (Q), wavelength (λ) and concentration of oleanolic and ursolic acids in the sample (C_{OA} and C_{UA}). All experiments were run at room temperature (20 °C).

Table 3.1: Operation conditions of HPLC for the selection of best mobile phase at 20 °C.

Mobile phase	Q (mL/min)	λ(nm)	C_{OA} (mg/mL)	C_{UA} (mg/mL)
Methanol				
MeOH/Water 95/5 (% v/v)				
Methanol/Water 90/10 (% v/v)		210		
ACN/MeOH 80/20 (% v/v)	0.4		0.0600	0.0895
ACN/MeOH 70/30 (% v/v)				
MeOH/n-Butanol 80/20 (% v/v)		215		
MeOH/2-propanol 80/20 (% v/v)		215		
Ethanol		218		

3.5 Breakthrough experiments

In this part of the experimental work, breakthrough curves were measured and thereafter the isotherm and mass transfer parameters were adjusted using Klinkenberg model. It was used Acclaim C30 column and the chosen eluent was methanol/water 95/5 (%, v/v).

3.5.1 Equipmental setup

The breakthrough experiments were conducted in a chromatographic unit that is installed in EgiChem laboratory of CICECO, as seen in Figure 3.3, which has tree pumps model Pump 100 and one pump Smartline Pump 1050. The pumps are from Knauer Pumps. The Acclaim C30 was the analytical column used (5 μm, 4.6 $\times$ 250 mm).

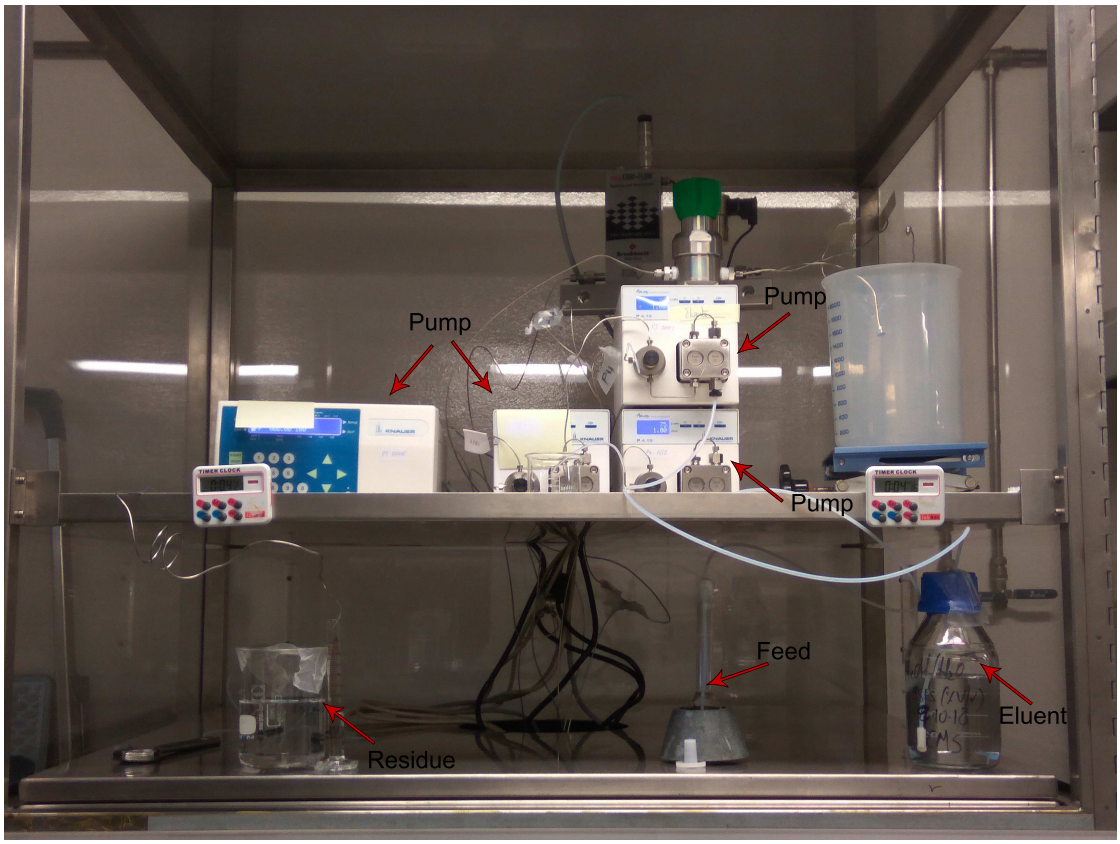

Figure 3.3: Equipment used for the breakthrough experiments.

3.5.2 Solution preparation

For the solution preparation, 129.7 mg of OA were weighted to prepare the initial solution in a 100 mL volumetric flask, which is completed with the eluent in study (methanol/water 95/5 (%v/v)). The diluted concentrations were made from this initial solution in 50 mL volumetric flasks, with 8, 20 and 30 mL , also completed with eluent. Ursolic solution and their diluted concentrations were preprepared similarly, with 203 mg of UA in a 100 mL and then 5, 20 and 35 mL. The concentrations of standards are presented in Table 3.2. The concentration C_0 was made for calibration purposes, making a dilution of concentration C_1 to half value.

Table 3.2: Concentrations of the diluted solutions of oleanolic and ursolic acids.

Acids	C_4 (mg/mL)	C_3 (mg/mL)	C_2 (mg/mL)	C_1 (mg/mL)	C_0 (mg/mL)
Oleanolic	1.297	0.778	0.519	0.208	0.104
Ursolic	2.030	1.421	0.812	0.203	0.102

3.5.3 Experimental procedure of breakthrough assays

The procedure was the following one:

1. Turn on the unit;
2. Set the adequate flow rate for the experiment;
3. Make the mobile phase flow through column by selecting the eluent pump;
4. Insert the vacuum in the flask and purge the system;
5. Allow to the system stabilize;
6. Switch on feed pump and start the experiment
7. Collect several samples of the outlet stream along time in Eppendorfs;
8. In order to regenerate the column, change to eluent pump;
9. Continue collecting samples of the outlet stream into Eppendorfs tubes, periodically;
10. Stop the pump;
11. Turn off the equipment.

The samples were gathered during process for future analysis in HPLC.

3.5.4 Operating conditions

The experiments with pure oleanolic and ursolic acids solutions were performed with a 1.0 mL/min flow rate and wavelength of 210 nm.

Breakthrough experiments were carried out for measuring adsorption isotherms of oleanolic and ursolic acids in a methanol/water 95/5 (%, v/v) mixture. For the data modeling it was used the Klinkenberg equation, which is applicable to linear systems, i.e. when isotherm is linear and when mass transfer is welll represented by the Linear Driving Force (LDF) model of Glueckauf. First, the breakthrough curves of pure oleanolic and ursolic acids were measured by sampling through time during the adsorption step. Adsorption was run until equilibrium and followed by column regeneration to recover the adsorbed acid, and quantify the solute in the solid phase.

3.5.5 Determination of breakthrough curves

The breakthrough curves were measured for the diluted concentrations $C_{\mathrm{OA},1} = 0.208$ mg/mL, $C_{\mathrm{OA},3} = 0.778$ mg/mL, $C_{\mathrm{UA},1} = 0.203$ mg/mL and $C_{\mathrm{UA},3} = 1.421$ mg/mL.

The collected samples for those concentrations were analyzed by HPLC in order to determined the triterpenic acid concentration and thus build the breakthrough curve. All samples were injected in HPLC following the procedure described in Section 3.4.2.

4 Results and discussion

4.1 Chromatographic assays for eluent selection

For evaluation of triterpenic acids separation, the parameters selectivity, resolution and retention are calculated by the Equations (4.1)-(4.3).

Retention factor (k') indicates how long it takes for a compound to exit the column. It can also be defined as the time for a particular compound to travel through the column until the detector. It is equal to the ratio of retention time of the analyte on the column ($t_{\mathrm{r,i}}$) to the retention time of a non-retained compound (t_0). When k' value is high, the sample is highly retained, interacting with the stationary phase [55].

$$k'_i = \frac{t_{r,i} - t_0}{t_0} \tag{4.1}$$

Resolution (R) is a quantitative measure of how well two elution peaks can be differentiated in a chromatographic separation. It is defined as the difference in retention times between the two peaks, divided by the combined half widths of the elution peaks $w_{1/2_1}$ [55].

$$R = 1.18 \times \frac{t_{r,2} - t_{r,1}}{w_{1/2_1} + w_{1/2_2}} \tag{4.2}$$

Selectivity ($\alpha_{i,j}$) can be defined as the ability of the system to chemically distinguish between sample components [55]. It is measured as a ratio of the retention factors (k') of the two peaks:

$$\alpha_{i,j} = \frac{k'_i}{k'_j} \tag{4.3}$$

When $\alpha_{i,j}$=1, k'_{i}=k'_{j} (equal retention times) and thus there is no separation.

The parameters of the C30 column were determined by injecting Uracil, a non retained compound frequently used in reversed phase columns and t_0 was 7.26 min at 0.4 mL/min flow rate.

For the eluent selection, 78 chromatographic experiments were performed, 26 of them were made with oleanolic and ursolic acids mixtures, and 52 involved only one triterpenic

acid in solution.

Table 4.1: Chromatographic study of the mixture separation of triterpenic acids (OA and UA).

Detector	Mobile phase (% v/v)	Q (mL/min)	tr_{OA} (min)	tr_{UA} (min)	k'_{OA}	k'_{UA}	α UA-OA	R_{UA-OA}
210 nm	MeOH	0.4	11.700	12.215	0.6116	0.6825	1.1160	1.2277
210 nm	MeOH/Water 95/5	0.4	14.685	15.710	1.0227	1.1639	1.1380	1.3590
210 nm	MeOH/Water 90/10	0.4	19.655	23.800	1.7073	2.2782	1.3344	1.7531
210 nm	MeOH/Water 90/10 + Acetic Acid	0.4	28.010	30.030	2.8581	3.1364	1.0973	2.2701
210 nm	MeOH/Water 95/5 + Acetic Acid	0.4	17.565	18.720	1.4194	1.5785	1.1121	2.0342
210 nm	ACN/MeOH 80/20	0.4	18.865	20.110	1.5985	1.7700	1.1073	1.8250
210 nm	ACN/MeOH 30/70	0.4	13.670	14.415	0.8829	0.9855	1.1160	1.5560
215 nm	MeOH/2-Propanol 80/20	0.4	-	-	-	-	-	-
215 nm	MeOH/Butanol 80/20	0.4	-	-	-	-	-	-
215 nm	Ethanol	0.4	-	-	-	-	-	-

Mobile phase in reversed phase HPLC usually consists of water or aqueous solutions and an organic modifier.

Ideal solvents exhibit as properties water-miscibility, low viscosity, low UV detection, good solubility properties and chemically are nonreactive. The most common organic modifiers are water, methanol and acetonitrile. Selecting the solvent is one of the most crucial parameters in an HPLC separation due to the effect it can have on the selectivity, the most effective tool for optimizing the resolution [56].

First, pure methanol was used as mobile phase. From the chromatographic experiment with pure methanol in Acclaim C30 (Figure 4.1), it is possible to conclude that the separation of the acids was not total and, according to Table 4.1, resolution and selectivity are low. Retentions factors of oleanolic and ursolic are, respectively, 0.61 and 0.68, which are bellow 1.

Next it was used mobile phases of methanol mixed with water. With methanol/water 95/5 (%, v/v) (Figure 4.2 (a)) and methanol/water 90/10 (%, v/v) (Figure 4.2 (b)) good results were obtained, with a resolution of 1.36 and 1.75 each and a selectivity of 1.14 and 1.33, respectively. It is notable that for higher percentage of water, higher are the retention times of acids, which is expected in advance as water is more polar and repels the hydrophobic analytes into the stationary phase, hence the retention times are long [56]. This is in agreement with the fact that the triterpenic acids are almost insoluble in pure water.

It is also worth noting the peak tailing in the chromatograms. The principle cause is due to the occurrence of more than one mechanism of analyte retention. The interactions with ionised silanols on the silica surface lead to peak tailing, so these interactions need to be reduced in order to achieve a good peak shape [57]. For that, it was added a little percentage of acetic acid (500 μL) to both mobile phases, lowering the pH. Results are represented in Figures 4.2 (c) and 4.2 (d) and show evident improvements in relation to the chromatograms of the non-acidified eluents (Figures 4.2 (a) and 4.2 (b)). When operating at a lower pH, secondary interactions can be minimized, due to the the full

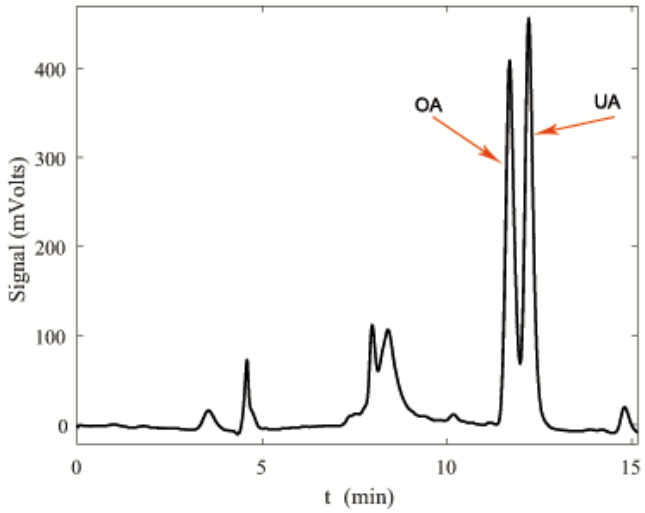

Figure 4.1: Chromatograms of oleanolic and ursolic mixture, using pure methanol as eluent and Acclaim C30 column. Chromatographic conditions: 0.4 mL/min flow rate, 210 nm wavelength and room temperature (20°C).

protonation of such ionisable residual silanol groups.

With addition of the acetic acid, it was observed an increase of the retention factors in both mobile phases as well as resolution, and the selectivity decreased in both cases, as seen in Table 4.1.

Then, chromatographic experiments with mixtures of acetonitrile and methanol as mobile phase were performed. Acetonitrile is often used due to its ability to solubilize many small molecules and its low viscosity [58].

With acetonitrile/methanol mobile phases full separation is achieved. For acetonitrile/methanol 30/70 (%, v/v) retention factors of 0.88 and 0.99 for oleanolic and ursolic acids were obtained, as well as selectivity 1.12 and resolution 1.56. For acetonitrile/methanol 80/20 % (%, v/v) gave rise to retention factors of 1.60 and 1.77 for OA and UA, selectivity 1.11 and resolution 1.82. Therefore, for a greater percentage of methanol, the retention time decreases (Figures 4.3 (a) and 4.3 (b)), which can be ascribed to the increment of OA and UA solubility.

Afterward, studies with 1-butanol, 2-propanol and ethanol have been conducted. Ethanol, 1-butanol and 2-propanol are polars. The polarity of the primary alcohols is inversely proportional to the number of methylene groups. 2-propanol, a secondary alcohol, is more commonly used as a modifier in normal phase chromatography but it may also be used for reversed phase due to its miscibility with a large range of different solvents. The 1-butanol and 2-propanol [59] possess high viscosity, which may lead to high pressure drops in the column. They are miscible with methanol, so mixtures of methanol/1-butanol and methanol/2-propanol 80/20 (%, v/v) were prepared.

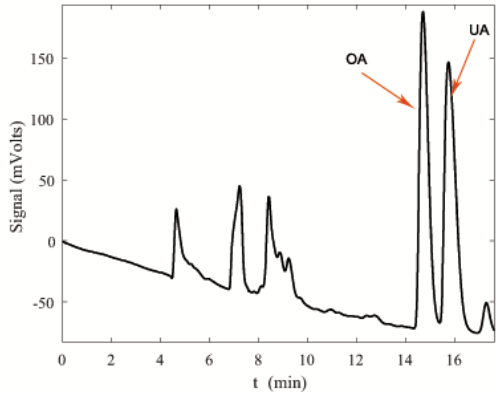

(a) Methanol/Water 95/5 (%, v/v)

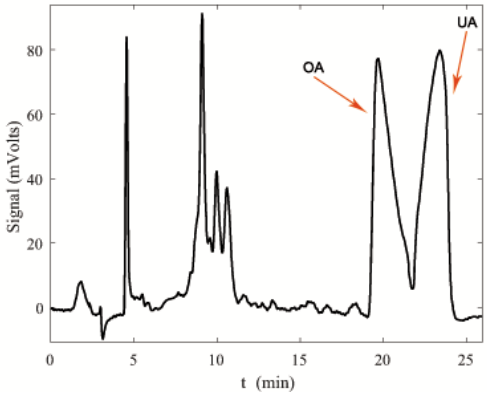

(b) Methanol/Water 90/10 (%, v/v)

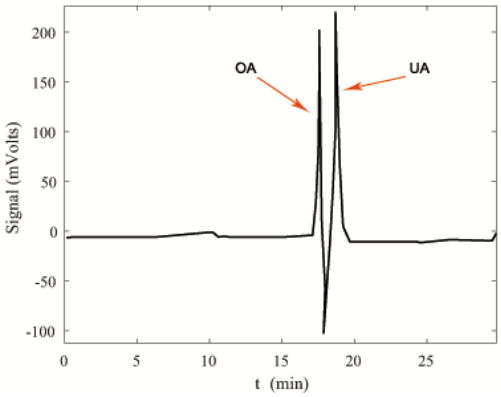

(c) Methanol/Water 95/5 (%, v/v) + acetic acid

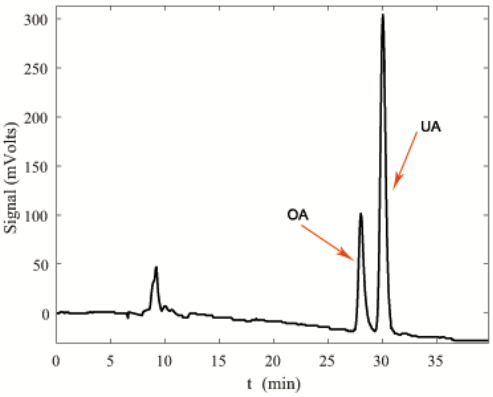

(d) Methanol/Water 90/10 (%, v/v) + acetic acid

Figure 4.2: Chromatograms of oleanolic and ursolic mixture, using methanol/water mixture as eluent and Acclaim C30 column. Chromatographic conditions: 0.4 mL/min flow rate, 210 nm wavelength and room temperature (20°C).

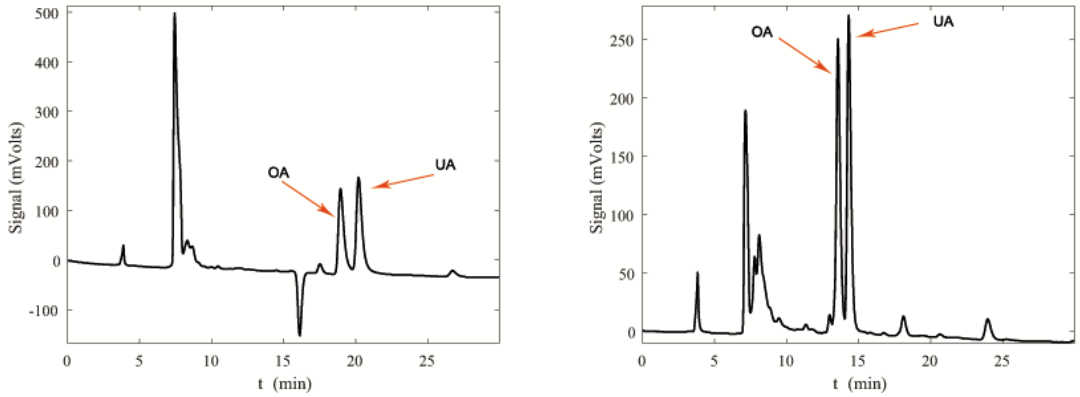

(a) Acetonitrile/Methanol 80/20 (% v/v)

(b) Acetonitrile/Methanol 30/70 (%v/v)

Figure 4.3: Chromatograms of oleanolic and ursolic mixture, using acetonitrile/methanol mixtures as eluent and Acclaim C30 column. Chromatographic conditions: 0.4 mL/min flow rate, 210 nm wavelength and room temperature (20°C).

The results obtained from the chromatographic experiments with methanol/1-butanol 80/20 (%, v/v) (Figure 4.4 (a)), methanol/2-propanol 80/20 (%, v/v) (Figure 4.4 (b)) and pure ethanol (Figure 4.4 (c)) were not acceptable as Figure 4.4 shows.

This can be explained by the UV cut-off of the solvents. UV Cut-off is the wavelength below which the solvent itself absorbs all of the light. In other words, it is the lower limit for the measurement in the UV-Vis spectrum. Once the triterpenic acids have low UV absorbency, and 2-propanol, 1-butanol and ethanol have between 210 and 220 nm, the oleanolic and ursolic acids were not detected by the equipment once wavelengths between 210 and 215 nm have been selected.

It is important to refer that for all studied solvents and solvents mixtures, the less retained compound was oleanolic acid and, consequently, the more retained one was ursolic acid.

The best results were obtained with methanol/water 95/5 (%, v/v), that was the selected mobile phase for the breakthrough experiments which are discussed in the following section.

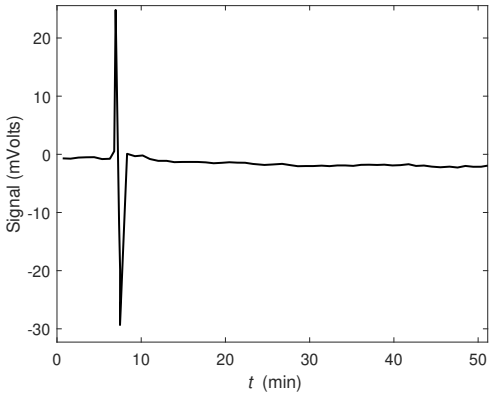

(a) Methanol/1-butanol 80/20 (% v/v)

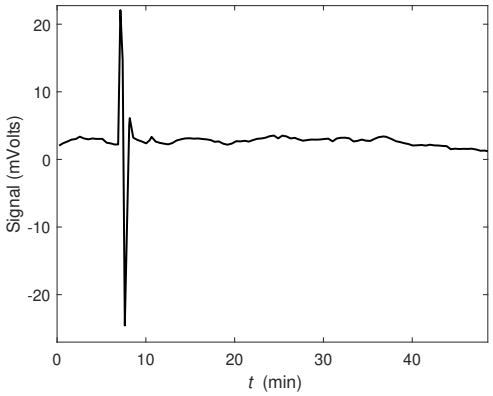

(b) Methanol/2-propanol 80/20 (% v/v)

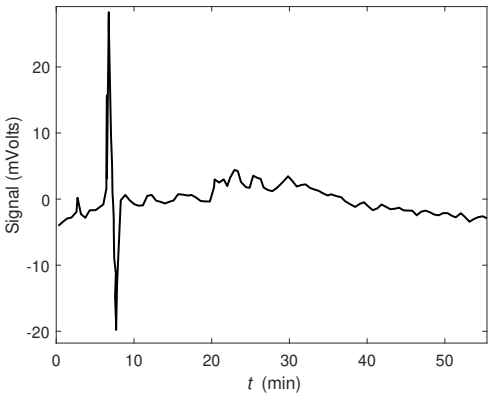

(c) Ethanol

Figure 4.4: Chromatograms of oleanolic and ursolic mixture, using methanol/1-butanol, methanol/2-propanol and pure ethanol as eluent and Acclaim C30 column. Chromatographic conditions: 0.4 mL/min flow rate, 210 nm wavelength and room temperature (20°C).

4.2 Determination of adsorption isotherms and transport parameters

In this section, the adsorption isotherms of oleanolic and ursolic acids were studied. It was always used methanol/water 95/5 (%, v/v), during the breakthrough experiments. Klinkenberg model (Equation 19 from section 2.3) was used for data modeling. This model is applied when the isotherm is linear and the mass transfer is well represented by LDF model (Linear Driving Force) and the axial dispersion is not relevant.

Breakthrough curves for oleanolic and ursolic acids, represented in Figure 4.5, were measured with samples collected through time. They were for each acid the concentrations $C_{\mathrm{OA},1}$ = 0.208 mg/mL, $C_{\mathrm{OA},3}$ = 0.778 mg/mL, $C_{\mathrm{UA},1}$ = 0.203 mg/mL and $C_{\mathrm{UA},3}$ = 1.421 mg/mL.

The experimental results were fitted with Klinkenberg model. For equilibrium, the fitted constants are $H_{\mathrm{OA}} = 2.06$ for oleanolic acid and $H_{\mathrm{UA}} = 2.16$ for ursolic acid. With relation to the global coefficient of mass transfer, the optimized values are $K_{\mathrm{LDF,OA}}$ = 30.48 min^{-1} for oleanolic acid and $K_{\mathrm{LDF,UA}}$ = 101.45 min^{-1} for ursolic acid. It is notable that the model is well adjusted to data points with an average absolute relative deviation ($AARD$) of 18.29 % and 26.88 % for oleanolic and ursolic acid, respectively. The average absolute relative deviation was calculated by:

$$AARD = \frac{100}{NDP} \sum_{i=1}^{NDP} \left| \frac{C^{calc} - C^{exp}}{C^{exp}} \right|_i \tag{4.4}$$

where superscripts calc and exp stand for calculated and experimental values and NDP is the number of data points.

Table 4.2: Optimized parameters of Klinkenberg model for oleanolic and ursolic acids.

Acids	H_{i}	$K_{\mathrm{LDF,i}}$ (min^{-1})	$AARD$ (%)
Oleanolic	2.06	30.48	18.29
Ursolic	2.16	101.45	26.88

4.3 Predicting the SMB performance of the separation of triterpenic acids

After the experimental selection of the adequate mobile phase and determination of the transport parameters of oleanolic and ursolic acids, it was made a prediction of a SMB unit performance for the isolation of those acids, using a program coded at EgiChem group (CICECO,UA).

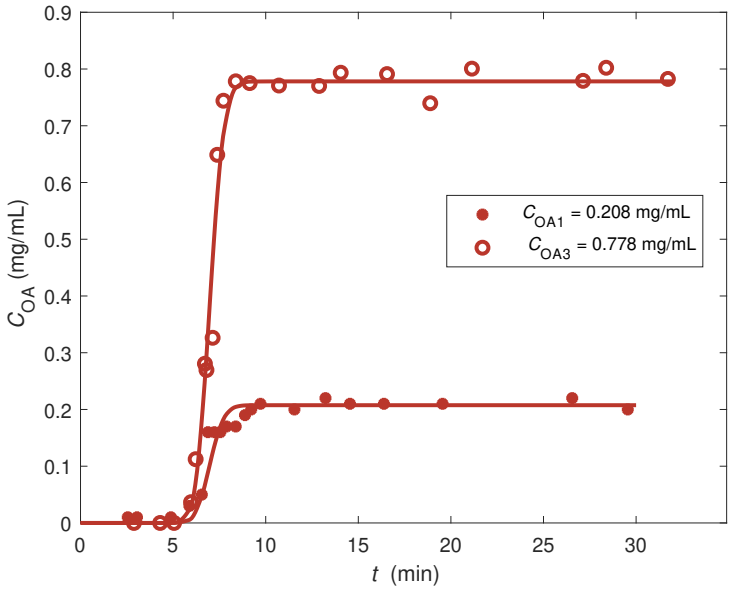

(a) Oleanolic acid breakthrough curves

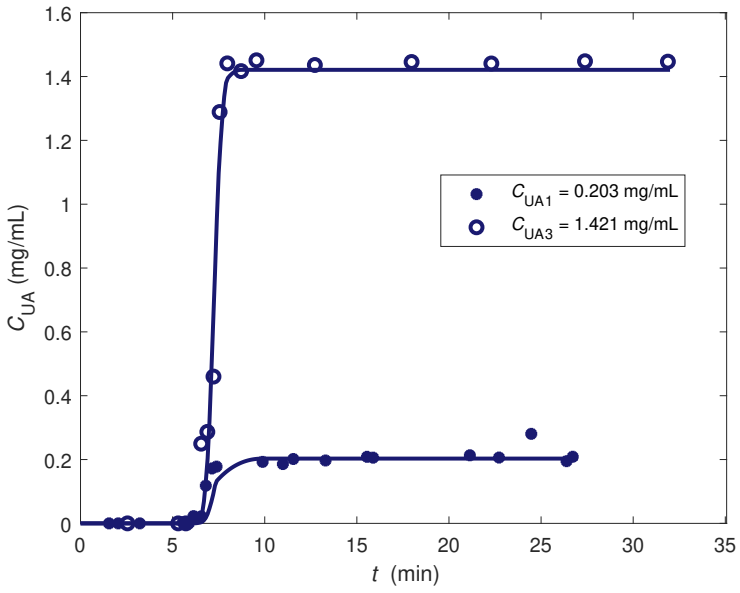

(b) Ursolic acid breakthrough curves

Figure 4.5: Adsorption breakthrough curves of oleanolic acid (a) and ursolic acid (b) at two different feed concentrations in Acclaim C30 column with methanol/water 95/5 (%, v/v) fed at 1 mL/min and UV detection of 210 nm, and room temperature (20 °C) Points - Experimental data, lines - Klinkenberg model.

It was consider that the disposition of the columns were 2-2-2-2, in other words, four sections with two preparative columns per section. It is relevant to say that all preparative columns possess the same characteristics.

It was used the triangle theory to determinate the ideal conditions and the optimal region of binary separation, which implies linear isotherms and null resistances to mass transfer and negligible axial dispersion. In order to calculate the flow rates, (referred in Chapter 2, Section 4), a value of ${Q^*}_{\mathrm{I}}$ was set, since the flow rate of section I is the highest of the unit. This value is calculated by using the Ergun (Equation 4.5). Its value was fixed to satisfy the maximum pressure drop allowed, which was consider 44 bar after adding a safety margin [18].

$$\frac{\Delta P}{L_{\mathrm{j}}} = \frac{150 {v_{\mathrm{oj}}}^* \mu_{\mathrm{f}} (1-\varepsilon_{\mathrm{b}})^2}{{d_{\mathrm{p}}}^2 \varepsilon^3} + \frac{1.75 \rho_{\mathrm{f}} {v_{\mathrm{oj}}}^{*2} (1-\varepsilon_{\mathrm{b}})}{d_{\mathrm{p}} \varepsilon_{\mathrm{b}}} \tag{4.5}$$

Here, ρ_{f} is fluid density, and ${v_{\mathrm{oj}}}^*$ is the superficial fluid velocity in the SMB.

Next, switch time (t^*) and solid flow rate (Q_{s}) are calculated by estimating β parameter, whose maximum value is 1.02, calculated using Equation 2.40 (Chapter 2). Since the flow rate in section I is higher, it preceded the calculation of the flow rates of the TMB unit, Q_{i}, starting by Q_{I}. The obtained values are presented in Table 4.4.

The SMB performance was evaluated using purity (Equation 2.46), productivity (Equation 2.49) and solvent consumption (Equation 2.48) as criterias. The axial dispersion was estimated on the basis of molecular diffusion coefficient ($D_{\mathrm{m,i}}$) and the flow around the adsorbent particles:

$$D_{\mathrm{ax,ij}} = 0.73 D_{\mathrm{m,i}} + 0.5 d_{\mathrm{p}} {v_{\mathrm{j}}}^* \tag{4.6}$$

where d_{p} is the adsorbent particle diameter and ${v_{\mathrm{j}}}^*$ is the interstitial fluid velocity in the SMB. The molecular diffusion coefficient was estimated using Wilke Chang equation[34]:

$$D_{\mathrm{m,i}} = 7.4 \times 10^{-8} \frac{T\sqrt{\phi M_f}}{\mu_f {V_{\mathrm{bp,i}}}^{0.6}} \tag{4.7}$$

where T is the absolute temperature (K), ϕ is a dimensionless association factor for the solvent, M_{f} is the molecular weight of the solvent in g/mol, μ_{f} is the solvent viscosity in cP, and $V_{\mathrm{bp,i}}$ is the solute molar volume at its normal boiling point (cm^3/mol) [18] estimated by:

$$V_{\mathrm{bp,i}} = 0.285 {V_{\mathrm{critical}}}^{1.048} \tag{4.8}$$

where V_{critical} is critical molar volume.

In Figure 4.6 a representation of the separation region (m_{II} vs. m_{III}) is shown for oleanolic and ursolic acids with methanol/water 95/5 (%, v/v). The estimated operating conditions of SMB unit are inside of optimal region of operation, where pure raffinate

Table 4.3: Parameters used in the simulation of the SMB unit

L_c (cm)	25
D_i (cm)	2.2
ε_b	0.356
Q^*_I (mL/min)	10
$K_{LDF,OA}$ (min^{-1})	30.48
$K_{LDF,UA}$ (min^{-1})	101.45
H_{OA}	2.06
H_{UA}	2.16
D_{ax} (cm^2/min)	4.7e-3
β	1.006

and extract are obtained. In Table 4.3, the parameters used in the simulator are listed, in order to obtain the region of separation by triangle theory.

As has been mentioned above, the simulations were carried out in order to assess productivity, *Prod*, solvent consumption, *SC*, and extract and raffinate purities, *PuX* and *PuR*, respectively. It was observed that cyclic steady state was reached at 40^{th} cycle of a total of 45 cycles. The performance parameters were then calculated from the 40^{th} cycle until the end of process.

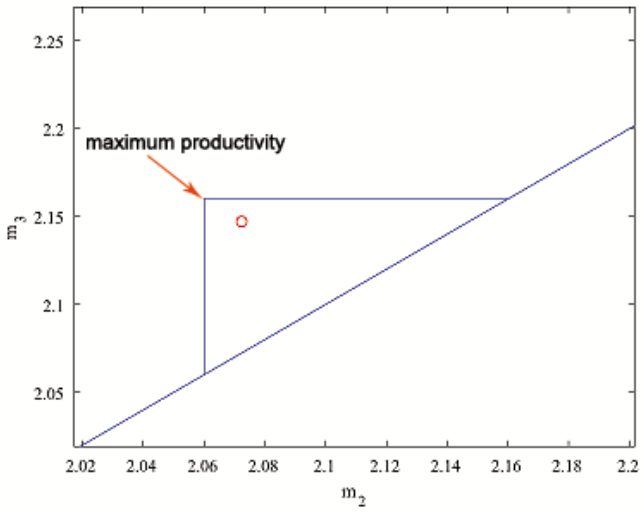

Figure 4.6: Graphical representation of the triterpenic acids separation with a mixture of methanol/water 95/5 (%, v/v). The vertex of the triangle represents the maximum productivity and the red circle represents the separation point.

The concentration history of oleanolic and ursolic acids through cycles, in the extract and raffinate streams, and average concentrations are given in Figure 4.7 and 4.8. The time of a complete cycle, t^*, is 16.68 minutes.

It is possible to separate these two acids and obtain purities higher than 99 % for

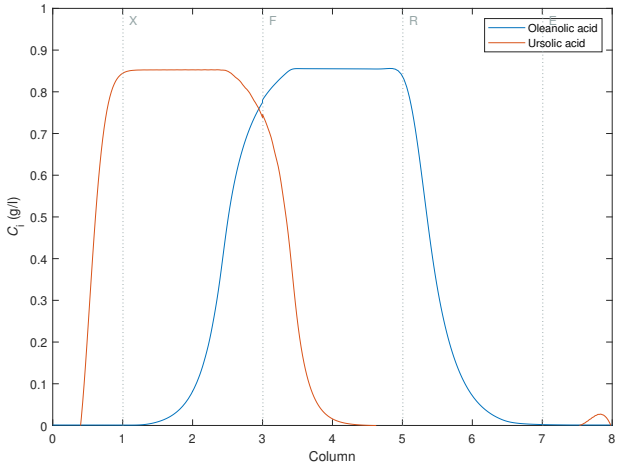

Figure 4.7: Concentration profiles of the most retained acid (ursolic) and the less retained acid (oleanolic) in a SMB with a 2-2-2-2 columns configuration, calculated under cyclic steady state (CSS).

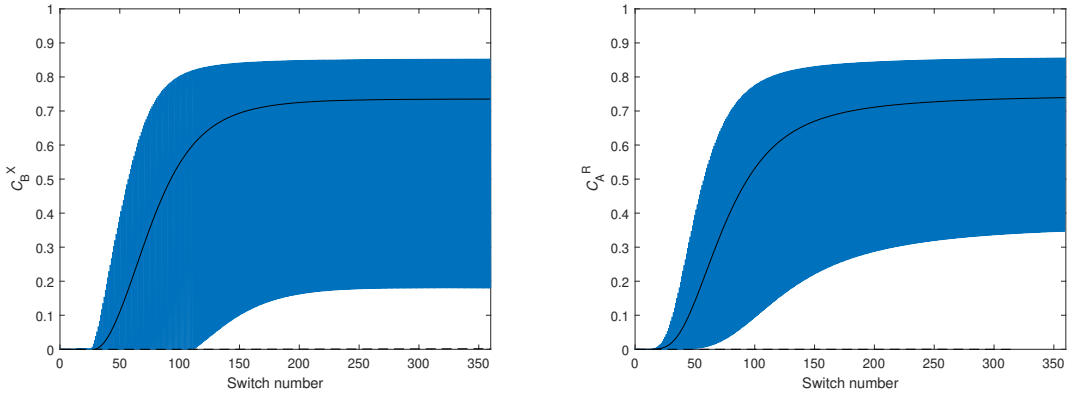

(a) Switch time average concentrations in extract together with ursolic acid concentration history.

(b) Switch time average concentrations in the raffinate together with oleanolic acid concentration history.

Figure 4.8: Simulation results at the end of the cycle of SMB operation, with cyclic steady state already established for the separation of oleanolic and ursolic acids from a binary mixture. The black line represents the average concentration.

Table 4.4: Parameters and flow rates values obtained from simulation.

x_{oa}	0.783
x_{ua}	0.722
Q^*_{II} (mg/mL)	9.631
Q^*_{III}(mg/mL)	9.905
Q^*_{IV} (mg/mL)	9.541
Q_{E} (mg/mL)	0.459
Q_{F} (mg/mL)	0.274
Q_{X}(mg/mL)	0.369
Q_{R} (mg/mL)	0.365
t^* (min)	16.68
PuR (%)	99.12
PuX (%)	99.89
SC (m^3/kg)	1.34
Prod ($\text{kg/m}^3_{\text{adsorbent}}$day)	1.04

both acids, as can see in Table 4.4, with a productivity of 1.04 kg/($\text{m}^3_{\text{adsorbent}}$· day).

The values obtained in the simulation are interesting since the purities of these compounds in chemical reagents providers are usually lower then 99%. This can be crucial for industries that have interests in the commercialization of these triterpenic acids.

5 | Conclusions and future work

Conclusions

In this work it was made a study of triterpenic acids separation, namely oleanolic and ursolic acids, by high performance liquid chromatography (HPLC) technique. The separation of the acids is complex due to their similar structure. In EgiChem laboratory (CICECO, UA) it is being installed a SMB unity, being pertinent to realize preliminary studies for the more adequate eluent selection and operating conditions.

It was analyzed the influence of solvents or mixture of solvents on the acids separation by measuring selectivities, resolution and retention factors.

In these studies it was used a C30 column, Acclaim C30, from Thermo Fischer Scientific, where the best results were obtained with mobile phase methanol/water 95/5 (%, v/v).

After solvent selection, it was carried out the study of the breakthrough curves of the acids in order to obtain the process parameters. For that, breakthrough experiments were performed and after that the collected data were fitted using the Klinkenberg model, which is applicable to linear systems. The obtained linear distribution coefficient of oleanolic and ursolic acids were, respectively, H_{OA}= 2.06 and H_{UA} = 2.16, and the global LDF coefficient of mass transfer were $K_{LDF,OA}$ = 30.48 min^{-1} and $K_{LDF,UA}$ = 101.45 min^{-1}. The model was well adjusted with $AARD$ of 18.29 % and 26.88 % for oleanolic and ursolic acids, respectively.

Finally, it was made a simulation in order to predict the performance of a SMB unit in a binary mixture separation, using a C30 preparative column fill, methanol/water 95/5 (%, v/v) as eluent, and 2-2-2-2 configuration (four section with two preparative columns each). The optimal conditions were obtained by triangle theory using several simulations with the main objective to obtain performance criteria like extract and raffinate purities, solvent consumption and productivity.

The cyclic steady state was attained at 40^{th} cycle of 45 cycles, reaching purities higher than 99 %. From the extract outlet we obtain ursolic acid with a purity of 99.89 % and from the raffinate outlet, the oleanolic acid was obtained with a purity of 99.12 %.

In conclusion, this master thesis demonstrates the viability of oleanolic and ursolic

acids separation through SMB, with higher purities than those found in the market, making these compounds available in many areas like pharmaceutical and nutraceutical industries.

Future work

Study the viability of oleanolic/ursolic acids separation by SMB, performing experiments in the lab unit that is almost installed in the EgiChem's laboratory.

For the same separation, accomplish tests with other column (C18 or C30) and/or using other solvent or mixture of solvents as mobile phases.

Simulate a modified SMB (*e.g.* Varicol, PowerFeed or ModiCon) as these can be more powerful than conventional SMB for binary mixtures of oleanolic and ursolic acids, or betulinic and oleanolic acids.

Simulate a PseudoSMB or a SMB cascade for the separation of a ternary mixture of betulinic, oleanolic and ursolic acids, once they appear frequently together in natural extracts.

Bibliography

[1] J. P. Aniceto, I. Portugal, and C. M. Silva, "Biomass-based polyols through oxypropylation reaction," *ChemSusChem*, vol. 5, no. 8, pp. 1358–1368, 2012.

[2] U. Fernandes and M. Costa, "Potential of biomass residues for energy production and utilization in a region of Portugal," *Biomass and Bioenergy*, vol. 34, no. 5, pp. 661–666, 2010.

[3] G. John, B. Vijai Shankar, S. R. Jadhav, and P. K. Vemula, "Biorefinery: A design tool for molecular Gelators," *Langmuir*, vol. 26, no. 23, pp. 17843–17851, 2010.

[4] J. H. Clark, R. Luque, and A. S. Matharu, "Green Chemistry, Biofuels, and Biorefinery," *Annual Review of Chemical and Biomolecular Engineering*, vol. 3, no. 1, pp. 183–207, 2012.

[5] A. R. Morais and R. Bogel-Lukasik, "Green chemistry and the biorefinery concept," *Sustainable Chemical Processes*, vol. 1, no. 1, p. 18, 2013.

[6] R. Domingues, A. Guerra, M. Duarte, C. Freire, C. Neto, C. Silva, and A. Silvestre, "Bioactive Triterpenic Acids: From Agroforestry Biomass Residues to Promising Therapeutic Tools," *Mini-Reviews in Organic Chemistry*, vol. 11, no. 3, pp. 382–399, 2014.

[7] R. M. A. Domingues, D. J. S. Patinha, G. D. A. Sousa, J. J. Villaverde, C. M. Silva, C. S. R. Freire, A. J. D. Silvestre, and C. P. Neto, "*Eucalyptus* biomass residues from agro-forest and pulping industries as sources of high-value triterpenic compounds," *Cellulose Chemistry and Technology*, vol. 45, pp. 7–8, 2011.

[8] R. M. Domingues, M. M. de Melo, E. L. Oliveira, C. P. Neto, A. J. Silvestre, and C. M. Silva, "Optimization of the supercritical fluid extraction of triterpenic acids from *Eucalyptus globulus* bark using experimental design," *Journal of Supercritical Fluids*, vol. 74, pp. 105–114, 2013.

[9] R. Da Silva Vieira, P. Canaveira, A. Da Simões, and T. Domingos, "Industrial hemp

or eucalyptus paper?: An environmental comparison using life cycle assessment," *International Journal of Life Cycle Assessment*, vol. 15, no. 4, pp. 368–375, 2010.

[10] CELPA - Associação da Indústria Papeleira, "Boletim Estatístico: Indústria Papeleira Portuguesa," 2016.

[11] M. M. de Melo, E. L. Oliveira, A. J. Silvestre, and C. M. Silva, "Supercritical fluid extraction of triterpenic acids from *Eucalyptus globulus* bark," *Journal of Supercritical Fluids*, vol. 71, pp. 71–79, 2012.

[12] R. M. Domingues, G. D. Sousa, C. M. Silva, C. S. Freire, A. J. Silvestre, and C. P. Neto, "High value triterpenic compounds from the outer barks of several *Eucalyptus* species cultivated in Brazil and in Portugal," *Industrial Crops and Products*, vol. 33, no. 1, pp. 158–164, 2011.

[13] L. Kong, S. Li, Q. Liao, Y. Zhang, R. Sun, X. Zhu, Q. Zhang, J. Wang, X. Wu, X. Fang, and Y. Zhu, "Oleanolic acid and ursolic acid: Novel hepatitis C virus antivirals that inhibit NS5B activity," *Antiviral Research*, vol. 98, no. 1, pp. 44–53, 2013.

[14] M. K. Lee, Y. M. Ahn, K. R. Lee, J. H. Jung, O. S. Jung, and J. Hong, "Development of a validated liquid chromatographic method for the quality control of *Prunellae Spica*: Determination of triterpenic acids," *Analytica Chimica Acta*, vol. 633, no. 2, pp. 271–277, 2009.

[15] H. Du and X. Q. Chen, "A comparative study of the separation of oleanolic acid and ursolic acid in *Prunella vulgaris* by high-performance liquid chromatography and cyclodextrin-modified micellar electrokinetic chromatography," *Iranian Chemical Society*, vol. 6, no. 2, pp. 334–340, 2009.

[16] F. Gbaguidi, G. Accrombessi, M. Moudachirou, and J. Quetin-Leclercq, "HPLC quantification of two isomeric triterpenic acids isolated from *Mitracarpus scaber* and antimicrobial activity on *Dermatophilus congolensis*, volume = 39, year = 2005," *Journal of Pharmaceutical and Biomedical Analysis*, no. 5, pp. 990–995.

[17] P. Yang, Y. Li, X. Liu, and S. Jiang, "Determination of free isomeric oleanolic acid and ursolic acid in *Pterocephalus hookeri* by capillary zone electrophoresis Ping," *Journal of Pharmaceutical and Biomedical Analysis*, vol. 43, no. 4, pp. 1331–1334, 2007.

[18] J. P. Aniceto, I. S. Azenha, F. M. Domingues, A. Mendes, and C. M. Silva, "Design and optimization of a simulated moving bed unit for the separation of betulinic, oleanolic and ursolic acids mixtures: Experimental and modeling studies," *Separation and Purification Technology*, vol. 192, pp. 401–411, 2018.

[19] L. O. Somova, A. Nadar, P. Rammanan, and F. O. Shode, "Cardiovascular, antihyperlipidemic and antioxidant effects of oleanolic and ursolic acids in experimental hypertension," *Phytomedicine*, vol. 10, no. 2-3, pp. 115–121, 2003.

[20] J. M. Castellano, A. Guinda, T. Delgado, M. Rada, and J. A. Cayuela, "Biochemical basis of the antidiabetic activity of oleanolic acid and related pentacyclic triterpenes," *Diabetes*, vol. 62, no. 6, pp. 1791–1799, 2013.

[21] L. Jie, "Pharmacology of oleanolic acid and ursolic acid," *Journal of Ethnopharmacology*, vol. 49, no. 2-1, pp. 57–68, 1995.

[22] X. H. Xu, Q. Su, and Z. H. Zang, "Simultaneous determination of oleanolic acid and ursolic acid by RP-HPLC in the leaves of *Eriobotrya japonica* Lindl.," *Journal of Pharmaceutical Analysis*, vol. 2, no. 3, pp. 238–240, 2012.

[23] J. Liu, Y.-F. Lu, Q. Wu, S.-F. Xu, F.-G. Shi, and C. D. Klaassen, "Oleanolic acid reprograms the liver to protect against hepatotoxicants, but is hepatotoxic at high doses," *Liver International*, no. March, pp. 1–13, 2018.

[24] G. Buckland, A. Pastor, L. Lujan-Barroso, C. A. Gonzalez, N. Travier, P. Amiano, J. M. Huerta, A. Agudo, C. Navarro, M. D. Chirlaque, M. J. Sánchez, M. Rodríguez-Barranco, A. Barricarte, E. Ardanaz, M. Dorronsoro, A. Molinuevo, J. R. Quirós, and R. de la Torre, "Determination of oleanolic acid in human plasma and its association with olive oil intake in healthy Spanish adults within the EPIC Spain cohort study," *Molecular Nutrition and Food Research*, vol. 61, no. 8, pp. 1–9, 2017.

[25] M. K. Shanmugam, X. Dai, A. P. Kumar, B. K. H. Tan, G. Sethi, and A. Bishayee, "Ursolic acid in cancer prevention and treatment: Molecular targets, pharmacokinetics and clinical studies," *Biochemical Pharmacology*, vol. 85, no. 11, pp. 1579–1587, 2013.

[26] L. López-Hortas, P. Pérez-Larrán, M. J. González-Muñoz, E. Falqué, and H. Domínguez, "Recent developments on the extraction and application of ursolic acid. A review," *Food Research International*, vol. 103, pp. 130–149, 2018.

[27] S. T. Cargnin and S. B. Gnoatto, "Ursolic acid from apple pomace and traditional plants: A valuable triterpenoid with functional properties," *Food Chemistry*, vol. 220, pp. 477–489, 2017.

[28] D. Kashyap, H. S. Tuli, and A. K. Sharma, "Ursolic acid (UA): A metabolite with promising therapeutic potential," *Life Sciences*, vol. 146, pp. 201–213, 2016.

[29] C. Romero, A. García, E. Medina, M. V. Ruíz-Méndez, A. de Castro, and M. Brenes, "Triterpenic acids in table olives," *Food Chemistry*, vol. 118, no. 3, pp. 670–674, 2010.

[30] R. Yin, T. Li, J. X. Tian, P. Xi, and R. H. Liu, "Ursolic acid, a potential anticancer compound for breast cancer therapy," *Critical Reviews in Food Science and Nutrition*, vol. 58, no. 4, pp. 568–574, 2018.

[31] "Oleanolic acid analytical standard | Sigma-Aldrich." https://www.sigmaaldrich.com/catalog/product/sial/42515?lang=pt{&}region=PT, [Accessed in 2018-11-08].

[32] "Ursolic acid analytical standard | Sigma-Aldrich." https://www.sigmaaldrich.com/catalog/product/sial/89797?lang=pt{&}region=PT{&}cm{_}sp=Insite-{_}-recent{_}fixed-{_}-recent5-2, [Accessed in 2018-11-08].

[33] A. Rajendran, G. Paredes, and M. Mazzotti, "Simulated moving bed chromatography for the separation of enantiomers," *Journal of Chromatography A*, vol. 1216, no. 4, pp. 709–738, 2009.

[34] J. P. Aniceto and C. M. Silva, "Preparative Chromatography: Batch and Continuous," in *Analytical Separation Science* (J. L. Anderson, A. Berthod, V. Pino Estévez, and A. M. Stalcup, eds.), pp. 1207–1313, Wiley-VCH Verlag GmbH & Co. KGaA., first ed., 2015.

[35] A. E. Rodrigues, *Simulated Moving Bed Technology: Principles, Design and Process Applications*. Elsevier Science, 2015.

[36] J. P. Aniceto and C. M. Silva, "Simulated moving bed strategies and designs: From established systems to the latest developments," *Separation and Purification Reviews*, vol. 44, no. 1, pp. 41–73, 2014.

[37] I. B. Nogueira, A. M. Ribeiro, M. A. Martins, A. E. Rodrigues, H. Koivisto, and J. M. Loureiro, "Dynamics of a True Moving Bed separation process: Linear model identification and advanced process control," *Journal of Chromatography A*, vol. 1504, pp. 112–123, 2017.

[38] M. Li, Z. Bao, H. Xing, Q. Yang, Y. Yang, and Q. Ren, "Simulated moving bed chromatography for the separation of ethyl esters of eicosapentaenoic acid and docosahexaenoic acid under nonlinear conditions," *Journal of Chromatography A*, vol. 1425, pp. 189–197, 2015.

[39] C. Y. Chin and N.-H. L. Wang, "Simulated moving bed equipment designs," *Separation and Purification Reviews*, vol. 33, no. 2, pp. 77–155, 2004.

[40] R. P. Faria and A. E. Rodrigues, "Instrumental aspects of Simulated Moving Bed chromatography," *Journal of Chromatography A*, vol. 1421, pp. 82–102, 2015.

[41] Science Direct, "ScienceDirect.com | Science, health and medical journals, full text articles and books.." https://www.sciencedirect.com/https://www.sciencedirect.com/science/article/pii/S0949328X08001798/pdfft?md5=a59c578fd88dd6dbb0f73c55ef83af25{&}pid=1-s2.0-S0949328X08001798-main.pdf{%}0Ahttps://www.sciencedirect.com/, [Accessed in 2018-10-18].

[42] J. Nowak, D. Antos, and A. Seidel-Morgenstern, "Theoretical study of using simulated moving bed chromatography to separate intermediately eluting target compounds," *Journal of Chromatography A*, vol. 1253, pp. 58–70, 2012.

[43] V. G. Mata and A. E. Rodrigues, "Separation of ternary mixtures by pseudo-simulated moving bed chromatography," *Journal of Chromatography A*, vol. 939, no. 1-2, pp. 23–40, 2001.

[44] C. A. Martínez Cristancho, S. Peper, and M. Johannsen, "Supercritical fluid simulated moving bed chromatography for the separation of ethyl linoleate and ethyl oleate," *Journal of Supercritical Fluids*, vol. 66, pp. 129–136, 2012.

[45] F. Denet, W. Hauck, R. M. Nicoud, O. Di Giovanni, M. Mazzotti, J. N. Jaubert, and M. Morbidelli, "Enantioseparation through supercritical fluid simulated moving bed (SF-SMB) chromatography," *Industrial and Engineering Chemistry Research*, vol. 40, no. 21, pp. 4603–4609, 2001.

[46] S. Jermann, S. Katsuo, and M. Mazzotti, "Intermittent simulated moving bed processes for chromatographic three-fraction separation," *Organic Process Research and Development*, vol. 16, no. 2, pp. 311–322, 2012.

[47] F. Wei, B. Shen, M. Chen, and Y. Zhao, "Novel simulated moving-bed cascades with a total of five zones for ternary separations," *Industrial and Engineering Chemistry Research*, vol. 51, no. 16, pp. 5805–5812, 2012.

[48] A. Seidel-Morgenstern, M. Schulte, and A. Epping, "Fundamentals and General Terminology," in *Preparative Chromatography: Second Edition*, pp. 7–46, 2005.

[49] J. D. Seader, E. J. Henley, and K. D. Roper, *Separation Process Principles - Chemical and Biochemical Operations*. Wiley, third ed., 2008.

[50] J. P. Aniceto, S. P. Cardoso, and C. M. Silva, "General optimization strategy of simulated moving bed units through design of experiments and response surface methodologies," *Computers and Chemical Engineering*, vol. 90, pp. 161–170, 2016.

[51] G. B. Cox, *Preparative Enantioselective Chromatography*. Blackwell Publishing Ltd, 2005.

[52] G. Zhong and G. Guiochon, "Analytical solution for the linear ideal model of simulated moving bed chromatography," *Chemical Engineering Science*, vol. 51, no. 18, pp. 4307–4319, 1996.

[53] Y. J. Choi, S. K. Han, S. T. Chung, and K. H. Row, "Separation of racemic bupivacaine using Simulated Moving Bed with mathematical model," *Biotechnology and Bioprocess Engineering*, vol. 12, no. 6, pp. 625–633, 2007.

[54] S. Gracin and Å. C. Rasmuson, "Solubility of phenylacetic acid, p-hydroxyphenylacetic acid, p-aminophenylacetic acid, p-hydroxybenzoic acid, and ibuprofen in pure solvents," *Journal of Chemical and Engineering Data*, vol. 47, no. 6, pp. 1379–1383, 2002.

[55] Barkovich, "High performance liquid chromatography - Chemistry LibreTexts." https://chem.libretexts.org/Textbook_Maps/Analytical_Chemistry/Supplemental_Modules_(Analytical_Chemistry)/Instrumental_Analysis/Chromatography/High_performance_liquid_chromatography, [Accessed in 2018-07-02].

[56] CHROMacademy, "The Theory of HPLC: Chromatographic Parameters," *CHROMacademy*, p. 23, 2014.

[57] Crawford Scientific, "Peak Tailing in HPLC." https://www.crawfordscientific.com/technical/chromatography-technical-tips/hplc-chromatography-tips/peak-tailing-in-hplcl, [Accessed in 2018-07-05].

[58] Shimadzu, "Tips for practical HPLC analysis - Separation Know How," *LC World Talk Special Issue*, vol. 2.

[59] S. Ball and K. Mapp, "Investigation into the Alternatives to Acetonitrile for the Analysis of Peptides on a SepTech ST150 10-C18," 2011.

[60] Dr. Deepak Bhanot, "Common Peak Shape Distortions in HPLC and their Prevention." http://lab-training.com/2014/01/17/common-peak-shape-distortions-in-hplc-and-their-prevention/, [Accessed in 2018-07-17].

[61] J. W. Dolan, "Why do peaks tail?," *LCGC Europe*, vol. 16, no. 9, pp. 610–613, 2003.

A Troubleshoot - Split peaks

Peak shape distortions are common and can appear by many causes such as pH of mobile phase, blockage due to particulate contamination, blocked frits and column overload [60].

During the experiments of this master thesis, peak shape distortions in diverse injections have been observed as represented in Figure A.1. This distortion is designated by split peak and occurs when a Gaussian peak gets a shoulder or twin and is an indication of degraded column performance. For improving the shape of such peaks several corrective steps were implemented [61].

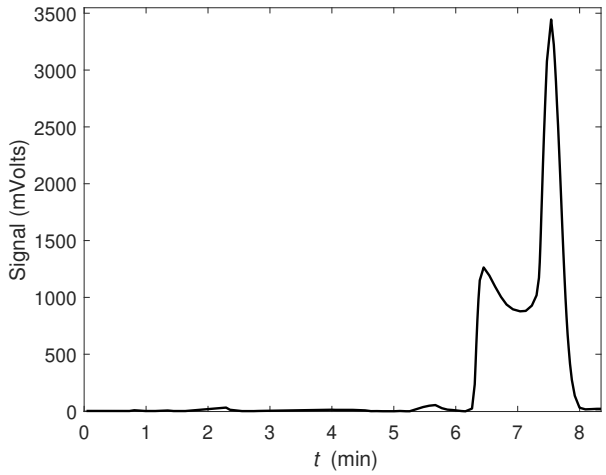

Figure A.1: A chromatogram with a split Peak

If only one peak of the a chromatogram is splitting or has a shoulder, the problem is likely to be something related to the separation. One way of checking this is to inject a smaller sample volume. If this results in two discernible peaks, the problem could be two components eluting close together. Revisiting the method parameters like mobile phase, temperature, flow rate or even column type are essential to improve the separation resolution [61].

The hypothesis of contamination of the mobile phase was discarded because a mobile phase methanol/water (95/5, %v/v) was prepared everyday. The first attempt to correct

the problem was to clean the column with a wash 100 % methanol and another wash with 100 % acetonitrile to remove strongly retained materials. The split peak persisted.

Next attempt was the preparation a new solution of oleanolic acid for further injection in HPLC. The problem continue, and also persists when a ursolic acid sample was injected, thefore was not the standards.

Then, it was used an UHPLC UltiMate 3000 from Thermo Fischer Scientific with the C30 column in study (Figure A.2). It was made an injection under the same conditions studied in the first HPLC (1 mL/min, 210 nm) and the peak was perfect. Hence the problem was not the column but something in the HPLC.

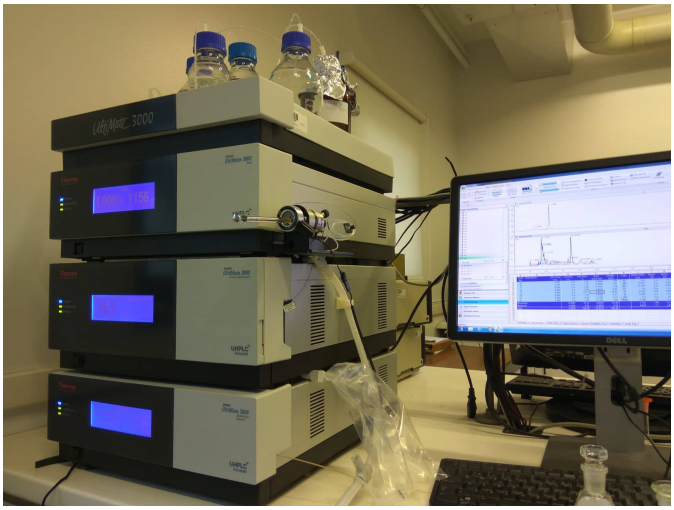

Figure A.2: UHPLC UltiMate 3000

Next, the column was back again installed in the original HPLC without the filter (Figure A.3) and an injection was performed, but the problem persisted.

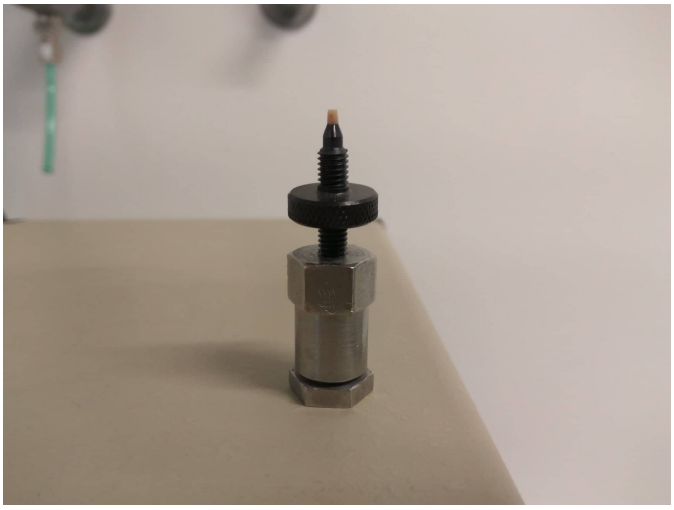

Figure A.3: In-line HPLC filter

Finally it was made a wash with isopropanol, and once has reversed the column and carried out a back-flush with solvent. It did not succeed, thus several injections were made with methanol and mobile phase. This fixed the problem and thus column was re-reversed and the filter was inserted again. The split peaks disappeared meaning that the problem was solved.